

**ACCEPTED MANUSCRIPT**

## Fish scale inspired structures - a review of materials, manufacturing and models

To cite this article before publication: Md Shahjahan Hossain *et al* 2022 *Bioinspir. Biomim.* in press <https://doi.org/10.1088/1748-3190/ac7fd0>

### Manuscript version: Accepted Manuscript

Accepted Manuscript is “the version of the article accepted for publication including all changes made as a result of the peer review process, and which may also include the addition to the article by IOP Publishing of a header, an article ID, a cover sheet and/or an ‘Accepted Manuscript’ watermark, but excluding any other editing, typesetting or other changes made by IOP Publishing and/or its licensors”

This Accepted Manuscript is © 2022 IOP Publishing Ltd.

During the embargo period (the 12 month period from the publication of the Version of Record of this article), the Accepted Manuscript is fully protected by copyright and cannot be reused or reposted elsewhere.

As the Version of Record of this article is going to be / has been published on a subscription basis, this Accepted Manuscript is available for reuse under a CC BY-NC-ND 3.0 licence after the 12 month embargo period.

After the embargo period, everyone is permitted to use copy and redistribute this article for non-commercial purposes only, provided that they adhere to all the terms of the licence <https://creativecommons.org/licenses/by-nc-nd/3.0>

Although reasonable endeavours have been taken to obtain all necessary permissions from third parties to include their copyrighted content within this article, their full citation and copyright line may not be present in this Accepted Manuscript version. Before using any content from this article, please refer to the Version of Record on IOPscience once published for full citation and copyright details, as permissions will likely be required. All third party content is fully copyright protected, unless specifically stated otherwise in the figure caption in the Version of Record.

View the [article online](#) for updates and enhancements.

# Fish scale inspired structures - A review of materials, manufacturing and models

Md Shahjahan Hossain, Hossein Ebrahimi, Ranajay Ghosh

Department of Mechanical and Aerospace Engineering, University of Central Florida.  
Orlando, FL

E-mail: rananay.ghosh@ucf.edu

March 2022

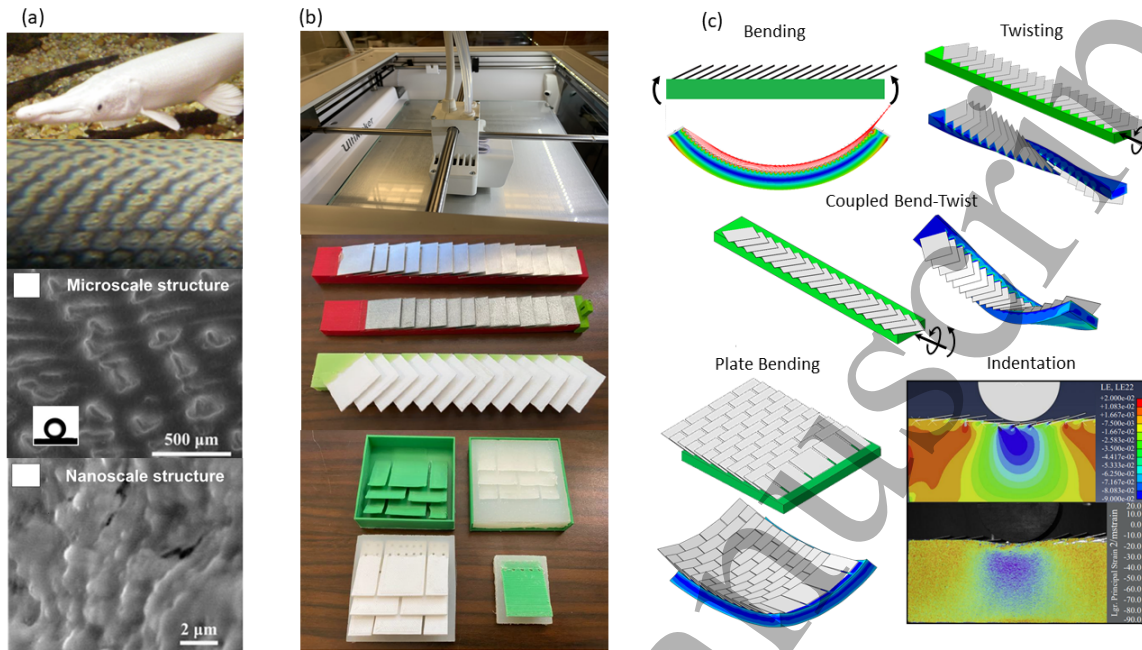
**Abstract.** Fish scales inspired materials platform can provide advanced mechanical properties and functionalities. These materials, inspired from fish scales take the form of either composite materials or multi-material discrete exoskeleton type structures. Over the last decade, they have been under intense scrutiny for generating tailorably and tunable stiffness, penetration and fracture resistance, buckling prevention, nonlinear damping, hydrodynamic and camouflaging functions. Such programmable behavior emerges from leveraging their unique morphology and structure-property relationships. Several advanced tools of characterization, manufacturing, modeling and computation have been employed to understand and discover their behavior. With the rapid proliferation of additive manufacturing (AM) techniques, and advancing envelope of modeling and computational methods, this field is seeing renewed efforts to realize even more ambitious designs. We present a review and recapitulation of the state-of-the art in fish scale inspired materials in this paper.

Key words: Biomimetics, Fish scales, Variable stiffness, Smart materials, Additive manufacturing (AM), Metamaterials

## 1. Introduction

Fish scale inspired structures have attracted considerable scrutiny over the past decade as high-performance materials platforms due to their promising mechanical and multifunctional properties. The fundamental origins of many of these properties lies on the intricate interplay of material and geometry of the scales at multiple length scales Fig. 1(a). The scales themselves are composite materials with intricate hierarchical organization of polymeric materials that provide resistance to damage and fracture.

At the same time, many other unusual properties arise at the structural length scale, which encompasses an array of scales, Fig. 1(b) . Such periodic arrays allow for scales interactions resulting in nonlinear strain stiffening, indentation resistance, locking, buckling resistance and anomalous frictional behavior. These later responses are primarily due to the emergent behavior arising from the intricate interactions between the periodically arranged plate-like scales on a deforming substrate Fig. 1(c) [1-7].

1  
2 *Biomimetic and Bioinspiration*  
3

26 **Figure 1.** From fish scales to engineering design. (a) Alligator Gar fish (adopted  
27 under CC BY 2.0) [8], and scales of Alligator Gar (adopted under CC BY 2.0) [9]  
28 (top), SEM images of the surface of fish scales at microscale and nanoscale structure  
29 level [10], (bottom). (owned by IOP) (b) 3D printer nozzle head and various types  
30 of biomimetic scales that were fabricated with the assistance of 3D printing [11]. (c)  
31 Different types of loading and scales engagement that can be considered for different  
32 analyses [11].

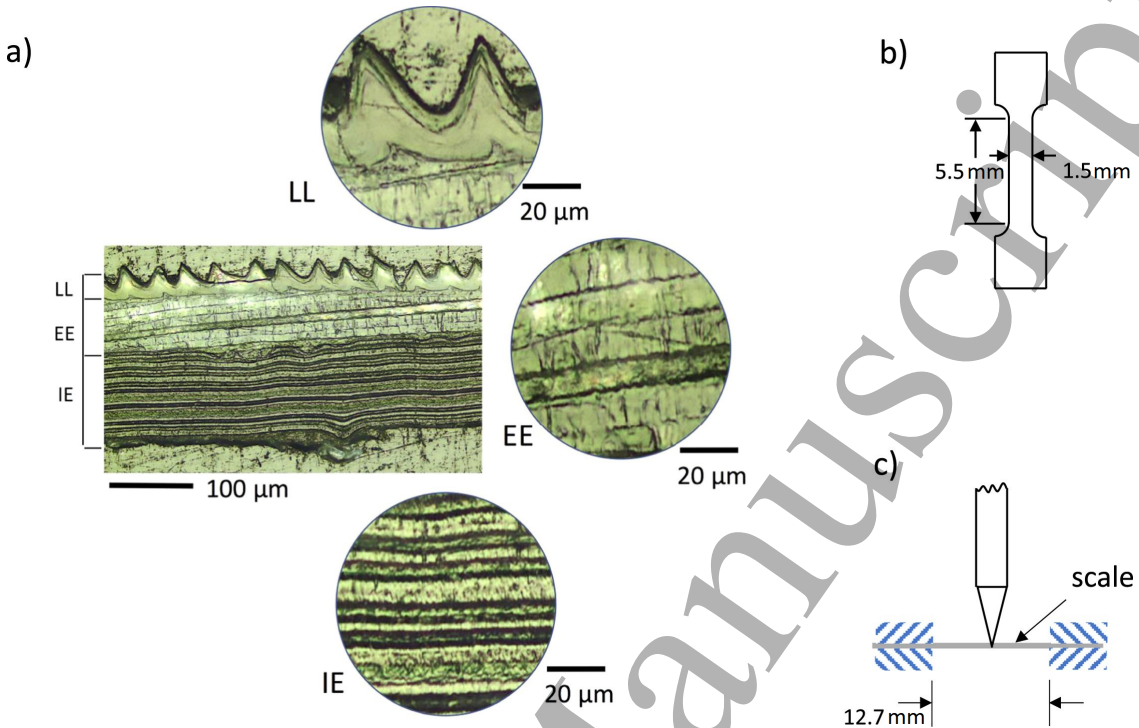
33  
34  
35 Two types of designs are possible – one where the scales are protruding from the  
36 surface Fig. 1(b), embedded partially on the substrate and the other where they are  
37 completely covered like composites. The partially embedded scale type design most  
38 closely mimics the actual scales of fish or reptiles [12–19]. In such cases, it is the sliding  
39 contact kinematics that leads to the most unusual nonlinear properties. Alternatively,  
40 other fish scale inspired composite-type designs also exist, where the scales are fully  
41 embedded within the top layer of the substrate [20–22]. Here, there is no explicit sliding  
42 between scales, but the stress profiles are altered on the top layer of substrate due to the  
43 constriction of the substrate's material between the stiff scales during loading [20–22].  
44  
45

46 Early interests in adopting scales for structural modifications were directed at their  
47 apparent armor-like functions, also observed in nature where the scales played a role in  
48 distributing the indenting force [23–27]. However, more recent efforts have expended  
49 towards a deeper understanding of the material behavior of the scales themselves [28–  
50 31] to design better materials [20, 22, 25], or to come up with “coatings” that prevent  
51 penetration [32]. Parallelly, efforts are underway for using scales’ sliding behavior to  
52 geometrically enhance the overall functions of the slender substrate [11, 33]. This can  
53 provide potential applications for smart structures and soft robotics due to variable and  
54 tunable stiffness. However, with ever expanding interests, many challenges arise typical  
55  
56  
57  
58  
59  
60

1  
2 *Biomimetic and Bioinspiration* 3  
34  
5 of a maturing field of materials. These include manufacturing, testing, modeling, and  
6 computations. Addressing these challenges are critical to enhance the potential of these  
7 structures and make their use more widespread.  
89 In this review, first we recapitulate the body of knowledge in mechanics and material  
10 properties of natural fish scales. We then highlight the route taken towards adopting  
11 the scales for enhanced structural properties that include nonlinear elasticity, drag  
12 reduction, and camouflage. Then, we discuss the advances in the fabrication and testing.  
13 Finally, we outline the advances made in the area of modeling and simulation. We  
14 conclude this paper by discussing the challenges and outlook in this area.  
1516  
17 **2. Mechanical characterization of natural fish scales**  
1819 Fish scales found in nature have hierarchical and heterogenous microstructures. These  
20 structural features are believed to be essential for their mechanically superior behavior.  
21 Typically studied scales in the biomimetic literature are of the types placoid, ganoid,  
22 elasmoid, dermal plates and scutes [34–37]. Placoid scales are found in cartilaginous  
23 fishes such as sharks and rays. Ganoids are peg-and-socket interlocking type scales  
24 with an outer layer of ganoine and typically of rhomboidal shape, typically with little  
25 overlap. They are found in fishes such as bichirs (Polypteridae), Bowfin (*Amia calva*),  
26 paddlefishes (Polyodontidae), gars (Lepisosteidae), and sturgeons (Acipenseridae).  
27 Elasmoid scales are thin, imbricated scales with a layer of dense, lamellar collagen  
28 bone (isopidine), underneath another layer of tubercles (typically composed of bone).  
29 Other popularly studied types include cycloid and stenoid types, which have significant  
30 overlap. A detailed description of scale type and morphology can be found in  
31 prior literature [38–40]. Various sophisticated imaging techniques have been used  
32 to study the microstructure of fish scales. These techniques include transmission  
33 electron microscopy (TEM), scanning electron microscopy (SEM), X-ray diffraction  
34 (XRD), Fourier-transform infrared spectroscopy (FTIR), CM-Toyoperal 650M column  
35 chromatography, and microcomputed tomography ( $\mu$ -CT). In this section we discuss  
36 the mechanical characterization of actual fish scales.  
3738 Early studies on Goldfish's scale discovered the structures of the constituent  
39 fibers electron microscopic analysis [41]. The microstructure of the elasmoid scales  
40 of *Carassius auratus* was analyzed using Philips EM 300 electron microscope with a  
41 cooled anticontamination device to find the microstructure of scales [42]. In another  
42 study by Zylberg et al. (1992), in-situ and in-vitro characterization was performed  
43 on the scales of *Carassius auratus L. (Cyprinidae)* to investigate the characteristics of  
44 fibrillar collagens of scales. The investigations were performed using electron microscopy,  
45 immunofluorescence, electrophoretic and HPLC analysis, immunoprecipitation, and  
46 RNA analysis. The authors outlined the influence of the environment on the actual  
47 fish scale's biological cell behavior, which effects the mechanical properties of the fish  
48 scales such as stress absorption and plastic deformation [43]. In a study by Giraud-  
49 Guille, et al. (2000) [44], fish scales were extracted from *Soleidae* flat fish, and imaging  
50

1  
2 *Biomimetic and Bioinspiration* 4  
34  
5 was done using X-ray diffraction, differential scanning calorimetry (DSC), polarized light  
6 microscopy, flow measurement, and transmission electron microscopy. This study, like  
7 a similar earlier study [45], was concerned with the biomedical application of fish scales  
8 from an amino acid perspective. Further studies have also been carried out focusing  
9 on the biocompatibility and potential bone regenerative properties of fish scales such  
10 as those of *Sparus aurata* [19, 46–48]. Similarly, fish scales and decalcified scaffolds  
11 collected from *Crisp flesh grass carps* were tested using SEM, FTIR, energy-dispersive  
12 X-ray spectroscopy (EDX or EDS), and tensile test. Also, the biodegradability of the  
13 scaffold has been examined to ascertain its potential for tissue regeneration [49].  
1415  
16 The compositional differences between fish scales were contrasted with porcine  
17 dermis using FT-Raman spectra on the scales of *Pagrus major* and *Oreochromis*  
18 *niloticas* [50]. The study used dehydrated and demineralized *Pagrus major*'s scales, and  
19 performed further characterization using SEM, TEM, EDS, FTIR, and tensile testing.  
20 Similar material properties were confirmed in later studies of *Pagrus major*'s scales  
21 [24]. An in-situ study on *Longnose gar* with the sequential alteration of scales was  
22 done for measuring the flexural stiffness, which influences the swimming condition [51].  
23 The hierarchical microstructure and electrochemical properties of *Longnose gar*'s scales  
24 were revealed with optical microscope, SEM, and EDS, which confirmed the potential  
25 application of such materials for high performance porous carbon material [52].  
2627  
28 In a study done by Feng et al. (2020), *Grass carp*'s scales were characterized using  
29 SEM, XRD, and atomic force spectroscopy (AFM), to reveal the lamellar structural  
30 arrangement of collagen fibers in the scales, and tensile test was done to determine their  
31 strength [53]. The authors reported that *Grass carp*'s scale matrix has a textured  
32 structure made up of several collagen sheets. Moreover, the matrix had excellent  
33 mechanical properties, in-vitro anti-enzymatic abilities, and compatibility with human  
34 corneal epithelial cells [53]. The study was done by a micro-CT scan to acquire the  
35 body dimension data, junction overlap, and body mineral density. In this study,  
36 Mercury porosimetry was performed to find the pore size distribution and volume  
37 percent porosity. SEM and micro-CT determined porous and sandwich structure. SEM  
38 and surface profilometry were used to characterize the interior and exterior surface  
39 topography. Moreover, back-scattered electron microscopy and energy dispersive X-ray  
40 analysis helped quantify the weight percent mineral content [54]. In-situ synchrotron  
41 small-angle X-ray scattering test was performed during the mechanical tensile tests to  
42 find out the deformation behavior of the collagen fibril lamellae in *Arapaima gigas*'s  
43 scales. This study showed that Bouligand-type structure of the fish scale contributes  
44 in the resistance against bending of the full scale and helps prevent fracture [55]. X-  
45 ray microcomputed tomography was used to generate digital 3D reconstructions of the  
46 mineralized scales of *P. senegalus* [56].  
4748  
49 Mechanical properties of *Cyprinus carpio*'s scales were also investigated by uniaxial  
50 tension experiment [57]. The authors found the tangent modulus (instantaneous  
51 modulus), strength, modulus of toughness, and strain to failure. The full-field  
52 deformation behavior was quantified by performing Digital Image Correlation (DIC).  
53

1  
2 *Biomimetic and Bioinspiration* 5  
34  
5 The authors also revealed the microstructures of fish scales using a series of sophisticated  
6 microscopies along with FTIR spectroscopy. This study found that fully hydrated head  
7 scales have twice strength than the tail scales, but the dehydrated scales do not have  
8 significant differences [57]. Similar study [58] was performed to find the mechanical  
9 properties of fish scales under tensile test, and the DIC and microscopic images showed  
10 that the tensile strength of carp's scales was dependent on the number of collagen  
11 fiber layers in their inner layers [58]. A black carp's (*Mylopharyngodon piceus*) scales  
12 was analyzed with tensile testing and DIC for finding the mechanical properties and the  
13 effects of different position (head or tail) of scales with its mineralization and dehydration  
14 [59].  
1516  
17 In another study [24], SEM, EDX, TEM, and FTIR were done to identify the  
18 properties including the chemical and physical properties of the mineralized and  
19 demineralized fish scales. Tensile strength measurement was undertaken where *Pagrus*  
20 *major*'s scales represented an average of  $93 \pm 1.8$  MPa and showed that the mineral  
21 content has significant impacts on the strength of fish scales. The tensile strength was  
22 measured using a texture analyzer (TA-XT2i; EKO) [24]. Tensile and puncture test on  
23 the scales were done by Ghods et al. (2019) [60], using a commercial universal testing  
24 machine, SEM analysis, and microCT. Furthermore, imaging of puncture test on the  
25 samples were conducted to analyze the dynamic loading response on elasmoid scales of  
26 *Cyprinus carpio*. This study found the significant difference in tensile properties, and  
27 puncture resistance among specimens from different locations in a fish (head, tail, and  
28 middle bodies), because of the differences in physical (such as thickness) and chemical  
29 properties (such as mineralized content). During the puncture test, the strain rate  
30 sensitivity was found to depend on the lamination and delamination properties of the  
31 microstructural layers. Details of the scale microstructure and the experimental methods  
32 shown in the figure 2 [60].  
3334  
35 Mechanical properties such as elastic modulus, ultimate tensile strength, strain at  
36 failure, modulus of toughness, and stiffness were also evaluated by uniaxial tensile test  
37 and transverse puncture test on the scales of *Cyprinus carpio* [61]. Here, scales were  
38 obtained from near the head, middle, and tail region of multiple fish, and then evaluated  
39 after fully hydrated in water or after exposure to a polar solvent (ethanol), for finding  
40 the effect of the polar solvent on the mechanical properties of scales. This study found  
41 that polar solvents can increase the resistance to failure of the scales, which is uncommon  
42 with the polar solvent in structural material [61]. In another study, tensile test, micro  
43 and nano indentation test (using a Vickers indenter), SEM, EDS, X-ray diffraction, and  
44 FTIR was done on *Arapaima Gigas*'s scales [62]. This study found the presence of amide  
45 I, II, and III, and characteristics and orientation of type I collagen can influence the  
46 mechanical properties such as tensile strength [62].  
4748  
49 SEM analysis and nanoindentation was also done on *Alligator gar*'s scale specimens  
50 to determine the interfacial geometric structure between ganoine and bone [63].  
51 Nanoindentation was performed to determine the elastic moduli's spatial variations and  
52 this nanoindentation data was also used to map the fish scale's cross-section, which shows  
53  
54

1  
2 *Biomimetic and Bioinspiration*  
3

28  
29 **Figure 2.** (a) Carp's scale cross-sections for representative head and tail scales with  
30 showing three principal layers: the limiting layer (LL), external elasmidone (EE) and  
31 internal elasmidone (IE). (b) Tensile testing specimen, which is a conventional dog-  
32 bone shaped tensile specimens, sectioned from the scales using punch and stamping  
33 process. (c) Clamped puncture testing sample schematic [60]. (Copyright permission  
34 has been adopted.)

35  
36 convergence of the elastic modulus for the ganoine and bone region. Additionally, SEM  
37 images of the microstructure and nanoindentation experiments qualitatively showed  
38 significant heterogeneity [63]. Scales of *C. Carpio* have been investigated with a puncture  
39 test (V-shape indenter) to find the flexural properties and the effectiveness of scales  
40 to resist puncture. In this study, nanoindentation test was performed on elasmoid  
41 and mineralized layers to determine the elastic modulus of each layer, and significant  
42 variation was found among the spatial scales. Thus, the scale distribution could be used  
43 in designing flexible puncture-resistant materials for instance in gloves. Both energy  
44 and load to puncture have significantly increased with the scale placed as a layer on top  
45 of the glove material [64].

46  
47 Further studies on perforation tests on the scales of a striped bass (*Morone saxatilis*)  
48 was done where it shows that the scales have high resistance to penetration. This study  
49 also observed the cause of high performance, which mainly is due to the fine balance  
50 between the stiffness and hardness of the outside layer as well as the softness and strength  
51 of the outer layer [65]. For this case study, the scale thickness was around 200-300 μm  
52 and perforation test was done with a sharp needle. In addition to the microstructure  
53 of the scales, puncture tests with a sharp needle (tip radius 35 μm) on the striped  
54 bass scales were performed to find the puncture resistance of the scales. The  
55 puncture resistance of the scales was found to be high, which is due to the high  
56 stiffness and hardness of the outer layer. The puncture resistance of the scales was  
57 found to be higher than the puncture resistance of the skin of the striped bass. The  
58 puncture resistance of the scales was found to be higher than the puncture resistance of  
59 the skin of the striped bass. The puncture resistance of the scales was found to be  
60 higher than the puncture resistance of the skin of the striped bass.

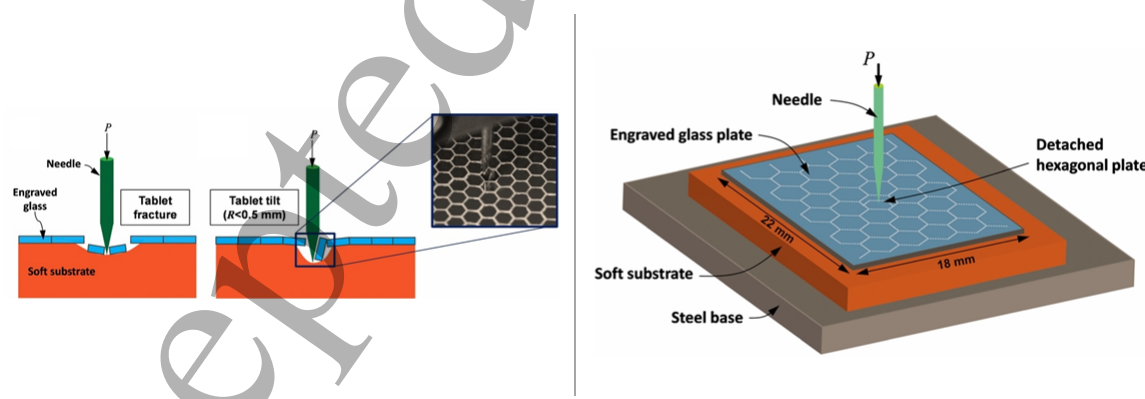
1  
2 *Biomimetic and Bioinspiration*  
3  
45 bass also highlighted the critical role of scales arrangement in enhancing the puncture  
6 resistance by distributing the force on the surface [66]. It was found that the individual  
7 scales provide a remarkable barrier against sharp puncture, although friction between  
8 the scales was negligible. Then, it was surmised that friction does not contribute to the  
9 increment of the puncture force [66]. Another penetration test on *Morone saxatilis* to  
10 replicate the biting attack with a sharp needle (tip radius  $\approx 30 \mu\text{m}$ ) confirmed that the  
11 presence of fish scales significantly increased the penetration resistance [67].  
1213 Another experimental investigation [68] with tensile testing, microstructure  
14 analysis, and Raman spectroscopy was done on the ontogenetic and regenerated scales of  
15 *C. Carpio*. Strength, modulus of toughness, and strain to fracture show the significant  
16 difference between the two kinds of scales [68]. An experimental study [69] was done  
17 to characterize the Arapaima's (*Arapaima Gigas*) scales through the penetration test,  
18 tensile test, in-situ SEM monitoring under tensile loading, small-angle X-ray scattering,  
19 and TEM test. This study has provided the details of the mechanism of deformation,  
20 delamination, and rotation of the lamellae, and showed how the scales restrict the  
21 penetration of external material or force [69]. The penetration resistance, which was  
22 measured by the instrumented nanoindentation technique, has been used to reveal the  
23 elastic and plastic properties of the scales [24]. An investigation was performed on the  
24 teleost fish skin to determine the role of skin bending through pinching test, and it was  
25 confirmed that the engagement of scales brought about a much higher bending resistance  
26 [17]. Tensile test, surface morphology, and microstructural analysis was made on five  
27 types of fish from the members of the family *Lutjanidae* to determine the mechanical  
28 properties and scales structure. It found that the mechanical performance of fish scales  
29 is influenced by the shape, array pattern, and compactness of strips on the posterior  
30 edges of a scale. This study helps to find the best structure for mechanical loading [70].  
3132 Interestingly, scales of *Labeo rohita* were studied to find the effect of Pb (II)  
33 biosorption and different pretreatment has been done before the analysis with FTIR  
34 spectroscopy. This study has been done by Nadeem et al. (2008) and found that  
35 pretreatment using HCl, H<sub>3</sub>PO<sub>4</sub>, and Ca(OH)<sub>2</sub> enhance the sorption capacity of fish  
36 scales, and pretreatment using H<sub>2</sub>SO<sub>4</sub>, NaOH, and Al(OH)<sub>3</sub> has reduce the sorption  
37 capacity. This study suggests that this fish scales could be an inexpensive solution for  
38 toxic metal sequestration [71]. All of the discussed experimental studies on different fish  
39 scales have been summarized in the Table 1.  
4041 In addition to scales, recent interests in suture-type structures have also increased.  
42 Suture interfaces are common in biological systems which is the connection of rigid or  
43 stiff elements (such as scales) by a compliant seam along the geometrically complex  
44 interfaces, with or without significant overlap among the stiff elements or scales. Suture  
45 structures are found in the exoskeletons of pangolin, armadillo, osteoderms, and boxfish  
46 [2, 72, 73]. Such structures have high resistance ability and flexibility without the  
47 critical decrease in stiffness and material strength [74–76]. Wang et al. (2016) studied  
48 the nanoscale suture structure found in the scales of different types of pangolin by  
49 optical microscopy, Fluorescence microscopy, SEM, TEM, micro-indentation, tensile  
50

1  
2 *Biomimetic and Bioinspiration* 8  
34  
5 **Table 1.** Summary of experimental studies done on different fish type and their  
6 findings, for the purpose of characterization of natural fish scale.  
7

Fish type	Experimental Method	Key Discoveries
Carassius Auratus [41–43]	Immunofluorescence, Electrophoretic, HPLC Analysis, RNA Analysis, and Immunoprecipitation	<ul style="list-style-type: none"> <li>- Influence of the environment on fish scale's biological cell was revealed.</li> <li>- The structures of the constituent fibers were revealed.</li> </ul>
Soleidae Flat Fish [44]	X-ray Diffraction, Differential Scanning Calorimetry (DSC), Polarized Light Microscopy, and Flow Measurement	<ul style="list-style-type: none"> <li>- Biochemical and biophysical properties were analyzed.</li> </ul>
Sparus Aurata [19, 46–48]	FTIR, TG–DTA Analysis, SDS–PAGE Analysis, and Polarized Light Microscopy	<ul style="list-style-type: none"> <li>- Biomedical application, biocompatibility and potential bone regenerative were analyzed.</li> </ul>
Crisp Flesh Grass Carps [49, 53]	FTIR, AFM, and Tensile Test	<ul style="list-style-type: none"> <li>- Potential use of tissue regeneration was revealed.</li> <li>- Mechanical properties and lamellar structure of scales were revealed.</li> <li>- In-vitro anti-enzymatic abilities and compatibility with human corneal epithelial cells were analyzed.</li> </ul>
Pagrus Major [24, 50]	FT-Raman Spectra, FITR, TEM, Tensile Testing, and Instrumented Nanindentation Technique	<ul style="list-style-type: none"> <li>- Material properties, chemical and physical properties were extracted.</li> <li>- Penetration resistance was studied to reveal the elastic and plastic properties of the scales.</li> </ul>
Oreochromis Niloticus [50]	FT-Raman Spectra	<ul style="list-style-type: none"> <li>- Chemical compositional differences with other fish scale were revealed.</li> </ul>
Longnose Gar [51, 52]	Stiffness Test	<ul style="list-style-type: none"> <li>- Flexural stiffness was measured, and confirmed the potential application for high performance porous carbon material.</li> </ul>
Arapaima Gigas [55, 62, 69]	In-situ Synchrotron Small Angle X-ray Scattering, Micro and Nano Indentation Test, Tensile Test, X-ray Diffraction, Penetration Test, FTIR, and In-situ SEM Monitoring under Tensile Loading	<ul style="list-style-type: none"> <li>- Deformation behavior of the collagen fibril lamellae was revealed.</li> <li>- Characteristics and orientation of type I collagen influence the mechanical properties.</li> <li>- Scales restrict the penetration by mechanisms of deformation, delamination, and rotation of the lamellae.</li> </ul>
P. Senegalus [56]	X-ray Microcomputed Tomography	<ul style="list-style-type: none"> <li>- Digital 3D reconstructions of mineralized scales were generated.</li> </ul>
Cyprinus Carpio [57, 60, 61, 64, 68]	FTIR Spectroscopy, DIC, Tensile Test, Puncture Test, MicroCT, Nanoindentation Test, and Raman Spectroscopy	<ul style="list-style-type: none"> <li>- Fully hydrated head scales have twice strength than the tail scales.</li> <li>- Mechanical properties differs among the scales of different place of body, and between ontogenetic and regenerated scales.</li> <li>- Polar solvents increase the resistance to failure and puncture, and flexural properties.</li> </ul>
Common Carp [58]	Tensile Testing and DIC	<ul style="list-style-type: none"> <li>- Tensile strength of carp's scales was found dependent on the number of collagen fiber layers in their inner layers.</li> </ul>
Mylopharyngodon Piceus [59]	Tensile Testing and DIC	<ul style="list-style-type: none"> <li>- Effects of different position (head or tail) of scales with its mineralization and dehydration on mechanical properties were analyzed.</li> </ul>
Alligator Gar [63]	Nanindentation	<ul style="list-style-type: none"> <li>- Interfacial geometric structure between ganoine and bone were revealed.</li> <li>- Spatial variations of mechanical properties were analyzed.</li> </ul>
Striped Bass (Morone Saxatilis) [65–67]	Perforation Tests, Puncture Tests, and Penetration Test	<ul style="list-style-type: none"> <li>- Fish scales shows resistance to penetration and puncture.</li> <li>- Stiffness and hardness of the outside layer as well as the softness and strength of the outer layer were analyzed.</li> <li>- Friction does not contribute to the puncture force increment.</li> </ul>
Teleost Fish Skin [17]	Pinching Test	<ul style="list-style-type: none"> <li>- The engagement of scales increased the bending resistance.</li> </ul>
Lutjanidae [70]	Tensile Test, and Surface Morphology	<ul style="list-style-type: none"> <li>- Mechanical properties of fish scales is influenced by the shape, array pattern, and compactness of strips on the posterior edges of a scale.</li> </ul>
Labeo Rohita [71]	FTIR Spectroscopy	<ul style="list-style-type: none"> <li>- This fish scales could be used as a solution for toxic metal sequestration.</li> </ul>
Gasterosteus Aculeatus [54]	MicroCT Scan, Mercury Porosimetry, Surface Profilometry, and BSEM	<ul style="list-style-type: none"> <li>- The study obtained the body dimension data, junction overlap, body mineral density, mineral content, and other physical properties of the scales.</li> </ul>
All Above Fish Types	Optical Microscope, Electron Microscope, SEM, EDS/EDX, and TEM	<ul style="list-style-type: none"> <li>- These experiments were done on different natural fish scales for finding the surface structure, microstructure, and chemical properties of fish scales.</li> </ul>

1  
2 *Biomimetic and Bioinspiration* 9  
34  
5 testing, and compression testing. It has been shown that the studied suture structure  
6 has interlocking behavior, improved bonding and shear resistance [2].  
78 In addition to fish, Pangolins possess striking scales pattern that must balance  
9 locomotion with protection. The fracture resistance of an African pangolin's scale is  
10 examined using three-point bend fracture testing in order to understand the toughening  
11 mechanisms [77]. In this study, the influence of material orientation and hydration  
12 level were examined, and other analyses were performed using a combination of  
13 optical and electron microscopy, and X-ray computerized tomography. The results  
14 showed that, similar to fish scales, the inherent structure of pangolin scales offers a  
15 pathway for crack deflection and fracture toughening [77]. Similarly, the pangolin  
16 scale's structure, mechanical properties, deformation, and damage behaviors were  
17 systematically investigated for finding the effect of hydration and orientation of scales.  
18 Hardness test, tensile test, and microscope analysis were done and found the properties  
19 of the scales varies with the orientation and hydration [78]. These studies have shown  
20 that the fundamental origins of enhanced behavior of fish scales are a result of complex  
21 microstructure as well as their action in concert with each other when impressed with  
22 external forces. These principles are essentially distilled to produce biomimetic materials  
23 with high performance.  
24  
25  
26  
27  
2829 **3. Biomimetic scale systems**  
3031 *3.1. Arrangement effects in biomimetic scales system*  
3233 The previous section outlined the critical importance of scale microstructure for high  
34 performance mechanical properties. Such microstructural topology can be used to design  
35 composites. For instance, a biomimetic Carbon Fiber Reinforced Polymer (CFRP)  
36 with a microstructure inspired by fish scales was designed and tested under the quasi-  
37 static indentation on a soft backing material [79]. This study showed that the design  
38 was effective in redistributing forces from a point load, thus improving its penetration  
39 resistance for the biomimetic fish scale structure [79]. The indentation resistance  
40 under quasi-static penetration testing was conducted on the replicated teleost fish skin  
41 [18]. Biologically relevant parameters of scale surface morphology, scale friction, and  
42 epidermal cover were changed in combination to assess their contribution to penetration  
43 resistance. Results from this research also suggest that optimized surface treatment can  
44 be applied to bioinspired fish skins to increase the resistance [18, 80].  
45  
4647 In addition to the microstructure of the scales themselves, their arrangement is  
48 also a critical parameter in the enhanced function of overall structure. It is well known  
49 that even within a single organism, scales distribution and shape changes with location  
50 reflecting their functions [81]. Here, the role of organized geometry comes into play,  
51 which leads to emergent mechanical behavior, like metamaterials [15].  
52  
5354 Indentation test and three-point bending test with cylindrical indenter were done  
55 to test the penetration resistance and flexibility, which can be used for finding the  
56  
57  
58  
59  
60

1  
2 *Biomimetic and Bioinspiration* 10  
34  
5 proper configuration of scale/substrate and material for the biomimetic armor [22]. The  
6 bending response of scaled and plain beams was measured by Instron universal testing  
7 machine. It was found that the stiffness of the scaled sample is higher, and even before  
8 the engagement of the scales due to the inclusion effect of scales [4]. Indentation studies  
9 on exposed scales sample were also carried out with 3D DIC for tracking the distribution  
10 of stress and strain across the samples along with comparisons with finite element (FE)  
11 modeling [82]. DIC revealed the global deformation and local contours of logarithmic  
12 strain fields in the composite design [20]. Stab-test was performed on the plain samples  
13 and scaled samples, which are similar to the knife penetration, and it found that scales  
14 samples were highly effective that can be suitable for body armor [83–85]. Another  
15 study was done focusing on the unstable tilting of individual scales subjected to off-  
16 centered point forces to enhance penetration resistance [86]. The puncture test was  
17 performed using two configurations, and pictures of the sample were acquired with a  
18 digital camera (Olympus Camedia C-5060) in micro-focus mode. The sample pictures  
19 were captured prior to the test to measure the offset distance accurately. Thereafter,  
20 images were captured at regular intervals during the test to monitor the tilt angles of  
21 the plate. Here, a failure mode was reported where the plate while remaining intact,  
22 suddenly tilts under the action of a localized force. The study found that the location  
23 of the point force on the plate, friction at the surface, size of the plate, and the stiffness  
24 of the substrate governs the stability of individual plates. A combination of scales with  
25 desired mechanical properties and these parameters can be used for optimal design [86].  
26  
2728 An indentation test was also performed for the puncture examination, where two  
29 types of radii were used for the indenters with quasi-static and static loading. From  
30 the test, it was found that the synthetic fish skin possessed many of the advantageous  
31 attributes of its biological counterpart. This underscores the possibility of obtaining  
32 an attractive combination of flexibility and protection found in natural materials with  
33 different combination scales and substrate [87]. Tensile test and three-point bending  
34 test were done on a biomimetic scales sample using an MTS Sintech machine. These  
35 tests evaluated the stability of the specimens which could be used as highly effective  
36 protection layers for wearable electronic devices and soft robotic [88].  
3738 Impact test was done on a biomimetic composite structure to verify the effects of  
39 helical stacking angle, which were found from an analytical model. It was observed that  
40 impact resistance decreases with the increase of helical stacking angle. SEM analysis  
41 was also done to find the relevant microstructure, which shows the biological structural  
42 effectiveness against the force for the composite structure (silicone and Kevlar fiber) [89].  
43 The biomimetic armor was tested under dynamic impact using an ElectroForce 3300  
44 equipment (TA Instruments), and ballistic test using a handgun. The sample design  
45 was inspired from the fish scale hierarchical structure (from one to six hierarchy levels),  
46 where the ultra-high-molecular-weight polyethylene (UHMWPE) was used as a base  
47 material. It has been discovered that these materials can absorb a higher level of energy,  
48 which are useful as high impact resistant materials [90]. The quasi-static and impact  
49 loading conditions were applied to the panels of biomimetic ceramic building blocks,  
50

1  
2 *Biomimetic and Bioinspiration* 11  
34  
5 which is having different interlocking angle where is placed on a aluminum frame. The  
6 panels' performance in terms of stiffness, strength, and energy absorption, improved  
7 with increasing the interlocking angle up to 20 degrees. The increased interlocking  
8 between the blocks, which restricted their relative motion were shown to be responsible  
9 for this [91].  
1011 In a study for assessment of bio-inspired stab-resistant armor, the test specimen  
12 was manufactured from a mix of virgin and recycled Duraform with different sizes and  
13 configurations, and it was stab-tested using an Instron 9250HV drop tower. All tests  
14 demonstrated successful levels of stab resistance, below the 7.00 mm permissible limit  
15 as defined by the CAST KR1 body armor standard, therefore validating the established  
16 body armor suitable for both survivability and maximum user mobility and comfort  
17 [84]. To study the 3D carved glass, biomimetic glass panels with different interlocking  
18 angles were studied using a universal testing machine (5 kN MTS Dual column loading  
19 stage). Additionally, the performance of the panels was assessed at high deformation  
20 rates by impacting them with a steel ball with the diameter equal to diameter of the  
21 ball used for the quasi-static tests. Deformation and fracture of the architectured panel  
22 were also shown to be a function of the geometry, size, arrangement of the blocks, and  
23 also of the degree of confinement imposed by the external frame [3]. Puncture tests were  
24 also performed to determine the resistance of the continuous glass (non-engraved) and  
25 engraved glass. The engraved glass was glued to the silicon rubber that was used as a  
26 substrate. It was found that the puncture resistance improved with a higher percentage  
27 in the engraved samples inspired from the fish scale compared to continuous plate. The  
28 technique of the testing sample is shown in figure 3 [92].  
2950  
51 **Figure 3.** Puncture test illustration on engraved samples, showing two possible  
52 condition, fracture and tilting (left), showing structure of engraved glass and shear  
53 of hexagon (right) [92]. (Already published and owned by IOP Publishing.)54 A test for finding the puncture resistance properties was done using an ABS  
55 needle, which leads to a small contact area. It is observed that scale-scale interactions  
56 significantly increase puncture resistance, while also decreasing flexural compliance.  
57 Some geometries and arrangement of scales have shown better performance than others.  
58 For instance, simple arrays show the worst performance and the geometry similar to the  
59

1  
2 *Biomimetic and Bioinspiration* 12  
3  
45 natural teleost and ganoid scales show the best performance [25]. The alumina scales  
6 with the soft substrate were tested using an MTS testing machine for the sharp needle  
7 puncture test with different combinations of the length of scales and overlap ratio. It  
8 was found that the size and overlap ratio affect the performance of the puncture test.  
9 The scaly skin is always stiffer than the silicone membrane, but more compliant than  
10 the continuous alumina strip. The samples were tested under a four-point bending  
11 configuration. The results demonstrate the capability of the proposed technique to  
12 cover large and complex surfaces, and it shows that the bio-inspired scaled skin can  
13 bend up to relatively large curvatures [93]. Earlier, for a fully embedded composite  
14 design of biomimetic scales, plane strain compression test was performed with varying  
15 geometric conditions, and the image of the test was captured by a DIC camera [20].  
16 The authors quantified the geometry and distribution of the embedded scales on the  
17 skin deformation behavior [20].  
1819 In addition to indentation studies, buckling experiments on a scaled skin were  
20 performed using a dual column universal testing machine (ADMET, Model eXpert 5000)  
21 to investigate the effects of biomimetic scales in the buckling modes and stability. The  
22 study found that scales can induce a stable mode II buckling which increases the overall  
23 flexural compliance and agility. The figure 4 shows the testing results of the buckling  
24 test to compare the experimental method and discrete element method (DEM) [94, 95].  
25 The scales themselves can also be tuned from stiff to soft using a stimulus sensitive  
26 material such as low melting point alloy (LMPA) [96]. Here, specifically engineered scales  
27 were used to design a metamaterial capable of transitioning from stiff to soft behavior.  
28 The samples were tested under three-point bending at various controlled temperatures.  
29 Results show the pronounced and reversible tunability in bending behavior and complex  
30 mechanical response in cyclical loading [96].  
3132 The influence of scales in tailoring the global deformation of slender substrates such  
33 as beams and plates are also of great significance for designing smart skins/structures  
34 and soft robotic structures [4–7, 12–14, 97]. Three-point bending experiments were  
35 performed using an MTS Insight machine on the scaled and unscaled samples to find the  
36 flexural response of the structure, and it demonstrated the differences in the stiffening  
37 response between scaled and unscaled samples, especially highlighting the dependence  
38 on the scale overlap ratio [4]. The stiffening response of scale-covered beam remains  
39 universal across bending of the uniformly distributed scales [4], bending of functionally  
40 graded scale in the scales spacing and in the initial inclination angles of the scales [14],  
41 and twisting of the uniformly distributed scales [6]. The experimental investigations  
42 showed a noticeable difference in deflection between uniform distribution of biomimetic  
43 scales and linear functionally graded scale-covered beam, under their own weight [14].  
44 Also for torsional loading, the effects of scales engagement were investigated using an  
45 MTS Bionix EM (Electromechanical Torsion 45 Nm), which showed significant stiffness  
46 gains in scale-covered beams in comparison with the plane beam [6]. Furthermore, this  
47 study discussed the significance of the scale's oblique angle with respect to the direction  
48 of the beam for twisting case as one of the most important differences between the  
49  
50  
51  
52  
53  
54  
55  
56  
57  
58  
59  
60

1  
2  
3  
4  
5  
6  
7  
8  
9  
10  
11  
12  
13  
14  
15  
16  
17  
18  
19  
20  
21  
22  
23  
24  
25  
26  
27  
28  
29  
30  
31  
32  
33  
34  
35  
36  
37  
38  
39  
40  
41  
42  
43  
44  
45  
46  
47  
48  
49  
50  
51  
52  
53  
54  
55  
56  
57  
58  
59  
60  
Biomimetic and Bioinspiration

13

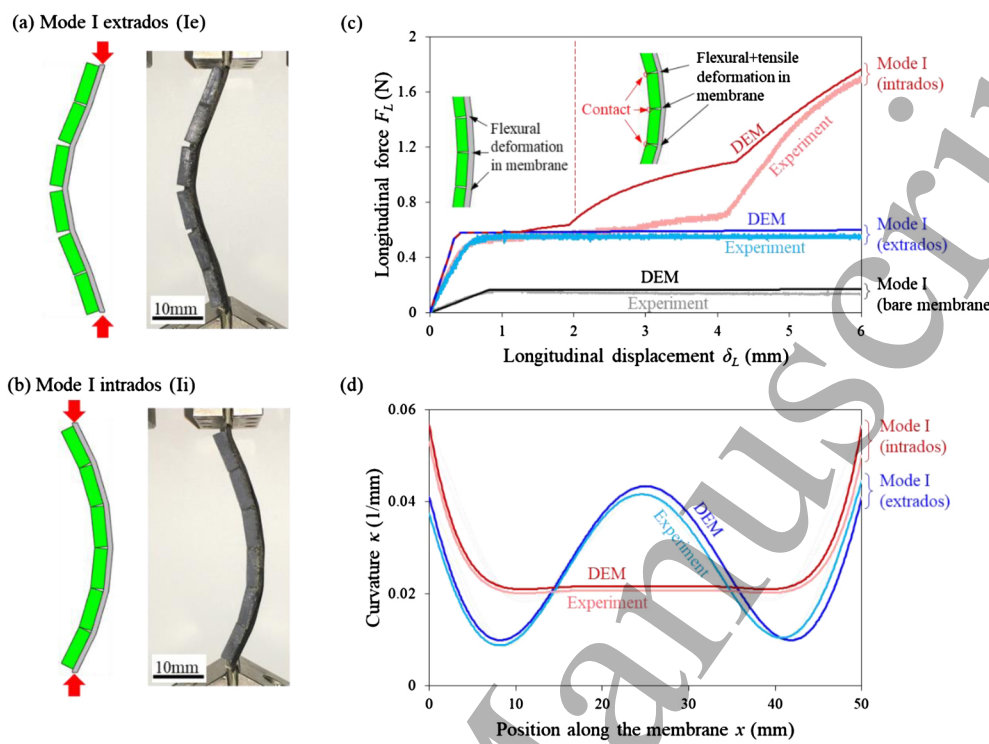


**Figure 4.** Experimental and DEM buckling test on a scaled polyurethane strip where the system buckles into (a) mode I-extrados and (b) mode I-intrados; (c) longitudinal force-longitudinal displacement curves showing a good agreement between the experimental and DEM results; (d) Curvature of the membrane as a function of the position along the membrane in the mode I-extrados and mode I-intrados configurations at loading point  $\delta_L = 6$  mm [94]. (Already published and owned by IOP Publishing.)

bending case and twisting case in 1D scale-covered beams [4, 6]. These studies outlined the highly non-linear, reversible, and tailororable properties of biomimetic scale-covered materials in both bending and twisting loads [4–7, 12–14, 97].

### 3.2. Surface effects in biomimetic scales system

In addition to mechanics, biomimetic shark skin has been tested inside a water tunnel for studying the drag reduction effect and found significant results [98]. The fish scales' superoleophobic properties have been studied using SEM and optical contact angle goniometers (OCA20). These artificial superoleophobic interfaces were manufactured from the inspiration of fish scales [99]. Biomimetic 3D printed fish scales were investigated to find their influence on the laminar-to-turbulent transition in the boundary layer of a laminar water channel. This study found the drag reduction properties of the surface, which can be used in bioinspired surfaces for flow control [100].

Wettability and drag reduction performance test using a pressure resistance test device was performed on a biomimetic fish scale Al-alloy sample to find the hydrophobic, superhydrophobic, low adhesion, and draft-reduction behavior. Microstructure of the

1  
2 *Biomimetic and Bioinspiration* 14  
34  
5 sample observed with SEM and the surface morphology was observed by laser confocal  
6 scanning microscope (LSM700-ZEISS-Germany) and ultra-depth of field microscope  
7 (SmartZoom5), and the 3d contour of the sample surface was obtained. This  
8 study provides an effective method for fabricating bionic fish scales, which provides  
9 superhydrophobic surface and drag reduction properties [101]. Biomimetic shark skin  
10 samples were tested to determine the hydrodynamic properties in both static and  
11 dynamic moving conditions in a controlled environment through robotic devices [102].  
12 The result shows that the effect of shark skin surface denticles on swimming performance  
13 relative to a smooth control is determined by the motion of the skin [102].  
1415  
16 Biomimetic skin based on shark skin were tested to determine the swimming  
17 performance. Two samples were prepared for this swimming performance test, one  
18 sample is based on ribbed rubber material and the other sample is based on the Speedo  
19 Fastskin®. It found that the biomimetic skin affects swimming performance [103].  
20 In addition, different bioinspired materials were also used for studying the surfaces  
21 with superhydrophobicity, superoleophobicity, drag reduction, and superhydrophilicity  
22 which can be used as self-cleaning material. The comparison was also done by different  
23 investigation techniques between different types of scales existing in nature [104–107].  
24 In a study by Bixler et al. (2013), the oil drag reduction on the actual fish scale and the  
25 biomimetic replica sample was measured for different kinds of natural scales. During  
26 the test, a sample was lined rectangular closed channels with the laminar oil flow, to  
27 evaluate the performance of the biomimetic structure [108].  
2829  
30 Fish scales surface properties such as surface friction has significant effect in  
31 biomimetic scales engagement. Friction can advance the locking envelope, significantly  
32 larger friction coefficient can create static locking condition [5]. In the dynamic study  
33 it is found that frictional effects can create viscous damping behavior [13]. Also, under  
34 twisting of the biomimetic fish scales systems, the Coulomb friction between the scales  
35 can lead to static locking condition [7].  
3637  
38 **4. Techniques and advances in fabrication of biomimetic scales**  
3940  
41 There are different technique for the fabrication of biomimetic fish scales. Among  
42 various technique, these can be divided into two main categories such as 3D printing  
43 assisted technique [109], and conventional manufacturing method such as stress-and-  
44 release fabrication [93] and laser cutting technique [92]. Depending on the requirement  
45 of the mechanical properties, implementation of the fabricated system, and testing  
46 requirement, different techniques are selected by the researchers [87, 92, 102, 110, 111].  
47 For high performance response, various parameters need to be controlled, such as size  
48 and shape of the scales, scale's aspect ratio, spacing between the scales, and scale angles.  
49 More significantly, the scales are often made of the same or different kind of materials,  
50 different sizes and shapes, which need to be attached to a substrate with much lower  
51 stiffness, requiring different joining techniques such as gluing. Fabrication of fish scale  
52 structures can be significantly leveraged by additive manufacturing (AM) due to the  
53  
54  
55  
56  
57  
58  
59  
60

Biomimetic and Bioinspiration

15

geometric nature of their organization. Despite this, several challenges remain unique to this system [26, 112, 113]. AM can also be used to fabricate different customized shapes, sizes, root geometry, and molds, which can be used to mimic various kinds of natural scales to endow tailorable properties. Since a combinatoric variety in the materials of scales and substrate can lead to a greater tailorability, multimaterial AM can be of special use. Multimaterial AM also removes the need of glues and complex mold making. In addition to AM, spraying technique is a new technique that can be introduced for the fabrication of biomimetic scales which is already studied for some other biomimetic applications [114–116].

#### 4.1. Techniques based on partial or full AM

Despite the wide range of scope of design in AM and ongoing work [117], there are still limits for the biomimetic design through this technology. In many cases, AM is used for the partial fabrication of the biomimetic parts [90, 109, 118–120]. An overview of AM manufacturing process, which are used currently, is shown in figure 5.

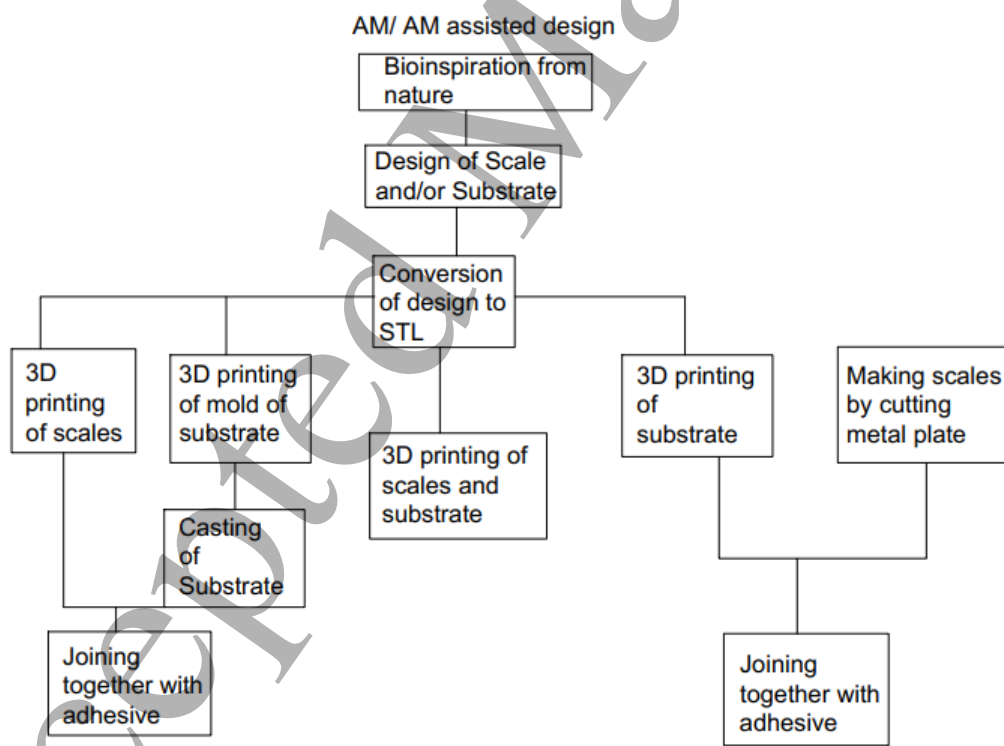


**Figure 5.** Typical AM assisted fabrication process flow of Biomimetic of fish scale.

Single material AM can be used in some parts of the biomimetic scale fabrication process. This typically involves either or both scales and mold fabrication using AM. When AM is used to create a mold for the substrate with groove-shape features for placing and inclusion of scales into the substrate, a soft polymeric resin such as silicone

1  
2 *Biomimetic and Bioinspiration* 16  
34  
5 can be poured in it and cured to obtain desirable substrate properties [121]. After the  
6 substrate is made with grooves, glue is used to attach the scales to the substrate. In  
7 an early study [122] in this field, the fabrication of biomimetic fish scale prototypes was  
8 done in few steps where 3D scanned biological geometry was initially achieved by micro-  
9 computed tomography scanning, then converted to surface mesh geometry, and finally  
10 converted to stereolithography (STL) file format for additive manufacturing. Then,  
11 using the scale-up of the design to avoid low wall thickness failure, an AM machine (or  
12 a 3D printer) was used for the fabrication of the scales [122].  
1314  
15 Inspired from the previous design techniques, multimaterial AM was used for the  
16 fabrication of the rigid (VeroWhite), and soft (TangoPlus) components separately.  
17 The ratio between the stiffness of materials selected for the scales and the substrate  
18 has significant effect on the mechanical behavior of the system [111, 122]. A similar  
19 approach was used with micro-CT scanning of samples, where 3D conversion of image  
20 data and modeling was done [102]. This study used multiple nozzle 3D printers to  
21 replicate different material properties with rigid and flexible structures and carefully  
22 consider the postprocessing of the 3D printed parts. Because of the limitation of the 3D  
23 printer for creating smaller parts, this technique created a scale-up denticle design [102].  
24 Another study also used micro-CT to acquire the shark denticle structure, which was  
25 then converted to an STL file optimized with Netfabb software to design the denticles'  
26 mold. Then this mold was used to fabricate the denticles, which at the end trimmed and  
27 manually assembled [123]. By using a multimaterial 3D printer, composite materials of  
28 the stiff plate (VeroWhite) and soft matrix (TangoPlus) prototype were fabricated with  
29 different inclination angles and volume fractions (between stiff phase and soft material)  
30 [22]. In another study, 3D printing of the scales and substrate was done separately and  
31 assembled using glue [124].  
3233  
34 Another method for fabricating biomimetic scales is by design and fabrication  
35 of a mold using 3D printing. Then this 3D printed mold can be used for making  
36 the flexible substrate. Finally, 3D-printed or non-3D-printed scales can be partially  
37 embedded into the structure with glue while keeping the required distance and overlap  
38 ratio [7, 14, 20, 82, 96, 121]. A typical fabrication process of biomimetic scales with mold  
39 and scales design is shown in Figure 6, including the mold and scales fabrication in 3D  
40 printer, substrate fabrication by adding curing agent, and finally insertion of scales into  
41 substrate.  
4243  
44 Another study [91] used a 3D printed block to create a silicon mold. Then a ceramic  
45 slurry (calcium sulfate powder + 19 wt % water) was pressure cast into the mold to  
46 create a ceramic building block, and finally the building block was tape transferred  
47 into the aluminum frame. The gap between the edges of the panel and the frame was  
48 filled with calcium sulfate paste to maintain uniform force transfer from the frame to  
49 the peripheral block. Here, the block was built with different inner and outer angles  
50 for material testing [91]. The scales were built with a high-resolution 3D printer,  
51 and the scales were then glued onto the surface of the polyurethane membrane using  
52 cyanoacrylate and with a gap of 0.5 mm between scales [94].  
53  
54  
55  
56  
57  
58  
59  
60

1  
2 *Biomimetic and Bioinspiration*  
3

17

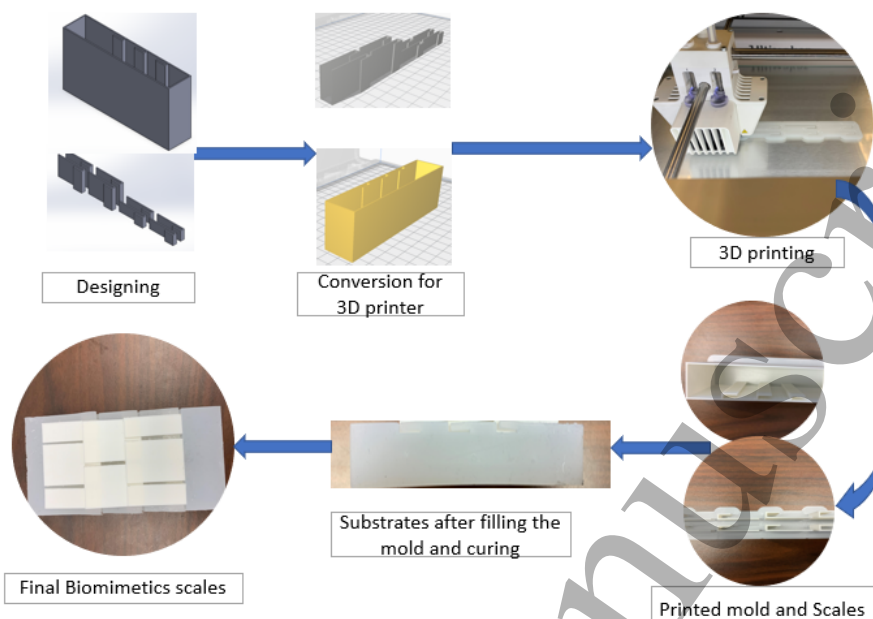


**Figure 6.** Fabrication process of biomimetic scales with molding concept.

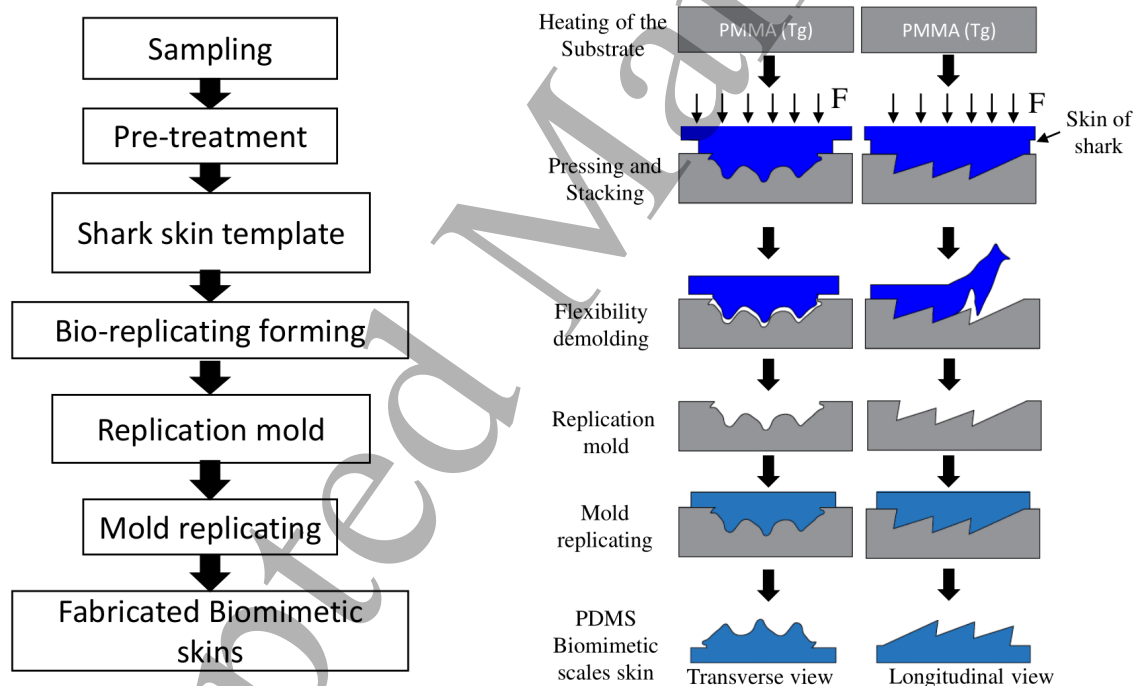
Laser-sintering 3D printing technique was used for fabricating armor, where the CAD model was transferred into the 3D printing machine and finally, additively manufactured samples were achieved [84, 85, 125]. Another technique described in literature is using the 3D printed scales (ABS photopolymer) fabricated with a direct light projector (DLP) printer [25]. After removing the support material, the array of scales was compressed using a biaxial vice system to minimize the gap between the scales, which was intentionally created during the 3D printing process. Then after gluing on the samples, the biaxial force was removed, and finally the scales were glued on a polyurethane membrane using adhesive [25]. A multimaterial 3D printer was used for the fabrication of biomimetic chiton scales, which started from the CAD design conversion to STL file and then transferring to the 3D printer. In this process, both soft and rigid materials were simultaneously printed at each layer [126]. For the study of scales effects on the body drag, biomimetic fish scale samples with different rows and thickness were made using 3D printed scales from CAD model directly [100]. Another approach was used where the substrate was 3D printed with soft material, and then the metallic scales were glued on the substrate [127].

#### 4.2. Other techniques

In this section, we discuss the techniques rather than AM-assisted methods. The shark skin (*Carcharhinus brachyurus*) [98] was chosen as the bio-replicated template with the proper treatment and the replication of the scales done with hot embossing with four steps: substrate heating, stacking and isostatic pressing, flexibility demolding, and mold replicating where polymethyl methacrylate (PMMA) flat plate was selected as

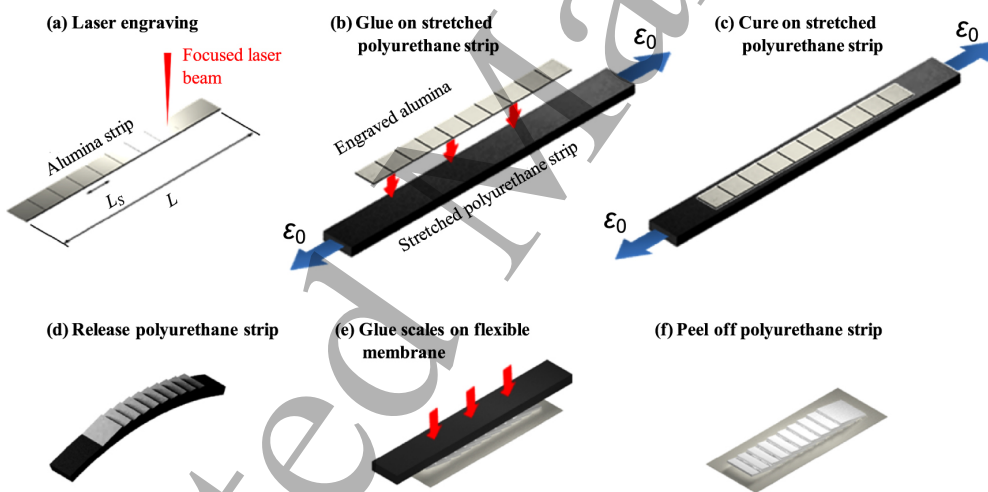
1  
2 *Biomimetic and Bioinspiration* 18  
3

4 the substrate. Mold replicating was done with a casting process where a specific ratio  
5 of curing agent was mixed and finally demolding provided the biomimetic skin. The  
6 manufacturing technique used the process flow shown in figure 7 [98]. Among the various  
7 fabrication method, molding [128] and hot embossing [98] are the two main techniques  
8 for fabrication of biomimetics shark skin. Compared with other manufacturing method,  
9 3D printing has many advantages. 3D printing makes multimaterial printing within  
10 a single step, also helps large area fabrication within a short period of time, and it  
11 allows denticles to be placed on the membrane accurately [102]. This technique also  
12 has controlled over the mechanical properties, size, arrangement of the scales, distance  
13 between the scales, and having undercut between denticle crown and the membrane  
14 surface. Despite all the advantages, 3D printing has one major disadvantage. Using  
15 current 3D printing technology, it is not possible to fabricate mako shark denticles that  
16 has complex surface characteristics of natural denticles [102].  
17  
18

47 **Figure 7.** Manufacturing process flow of biomimetic shark skin [98].  
48

49 A similar casting technique was used to fabricate the biomimetic fish scales,  
50 where polydimethylsiloxane (PDMS) precursor liquid was mixed with the curing  
51 agent for creating the template, and finally fish-scale structures were made from the  
52 polyacrylamide hydrogel films [99]. For designing a biomimetic armor, rigid protective  
53 plates (glass) with defined size and shape are placed over a soft substrate (flexible  
54 rubber), and this was achieved by laser engraving technique on the glass to gain the  
55 natural protective system characteristics [92].  
56  
57

58 The laser engraving technique is also used with interlocking mechanism inspired  
59  
60

1  
2 *Biomimetic and Bioinspiration* 19  
34  
5 by nature-like fish scales on the glass, for increasing the impact resistance of the glass  
6 surface. The engraved glass panel was separated and finally put into the aluminum frame  
7 for making the samples ready for testing [3]. The synthetic fish skin material has been  
8 designed to duplicate the material properties of teleost fish skin consisting of leptoid-  
9 like scales. Rectangular scales with fixed size were cut with a controlled mesh from a  
10 large cellulose acetate butyrate sheet. The scales were inserted into a polypropylene  
11 netting with one-half of scale under the mesh, and finally they were connected with  
12 three stitches and a single knot with prefabricated holes [87].  
1314  
15 A unique technique was developed where the alumina strip (used as a row of scales)  
16 was engraved using a focused laser beam [93]. This engraved alumina was glued to a  
17 pre-stretched polyurethane strip, and after releasing the stretch of strip, the scales slide  
18 on each other and make an overlap pattern of scales. Then, the prepared overlapped  
19 scales pattern was glued on a flexible membrane, and finally the polyurethane strip  
20 peeled off to obtain the flexible armor-like structure. This step-by-step fabrication has  
21 been shown in figure 8 [93].  
2246  
47 **Figure 8.** Stretch-and-release step by step fabrication of biomimetic scales [93].  
48  
49 (Already published and owned by IOP Publishing.)50  
51  
52  
53  
54  
55  
56  
57  
58  
59  
60 In a recent study, inspired from carp's (*Cyprinus carpio*) scales, the nylon sheet was laser cut and a silicon substrate was cast over scales, which was embedded in the female mold of substrate. After the demolding, the scales were embedded in the substrate, and the final sample was achieved for testing [80]. For creating hierarchical structural materials, ultra-high-molecular-weight polyethylene (UHMWPE) plates (as base material) and fibers were used for the manufacturing of protecto-flexible (Pf) armor in different configurations ranging from monolithic (one level of structural hierarchy H-1) up to six levels of structural hierarchy (H-6). This was specially prepared with a specific fabrication process (described in the supplemental material of [90]), and finally these samples were cut with laser engraving for the preparation of the hierarchical structure. The structure of this newly constructed material resembles the geometrical patterns

1  
2 *Biomimetic and Bioinspiration* 20  
34  
5 found in armadillo's osteoderms and the flexible impact-tolerant configuration found in  
6 fish scales [90].7 In a bioinspired armor design [79], a perforation resistant carbon fiber reinforced  
8 polymer (CFRP) was developed inspired from the ratios in teleost fish skin. This  
9 CFRP composite structure is consisted of the quasi-isotropic laminated base plate  
10 and cross-ply scales configuration. Rows of scales were sequentially attached to the  
11 base plate, having 1.5 mm inserted into the base plate, and placing a nonstick film  
12 between each layer of the scales to keep them separated during curing [79]. A different  
13 method was carried out for fabricating by using decellularized and decalcified fish scale  
14 derived scaffolds. Three different kinds of scaffolds were made by using decellularization  
15 and decalcification treatments. This samples were used to test the usability for tissue  
16 regeneration engineering [49]. Biomimetic flexible composite structures using silicone  
17 (silicon with curing agent) and Kevlar fibers were made firstly by mixing both the  
18 composite materials. Then, vacuum pump was used for removing the air bubbles, and  
19 after pouring the required amount of material into a rectangular mold, again vacuum  
20 was used for more assuring of removing the bubbles. After that, the mold is placed in  
21 the oven for curing. In next step, Kevlar fibers were included in the solidified mold,  
22 covered it with another part of the mixture, and repeated the same curing process. Each  
23 sample had five layers of fibers and had a constant helical angle [89].  
2425 Aluminum alloys were used as the base material to fabricate the biomimetic oblique  
26 groove structure of *Sciaenops ocellatus*'s scale. The process was started with the  
27 electrical discharge machining (EDM) cut for cutting the Aluminum alloy, then a  
28 laser device (YLP - ST20E) was used for fabricating the multiple curves on the scales.  
29 Finally, the samples postprocessing was done using ultrasonic cleaning and drying [101].  
30 Polydimethylsiloxane (PDMS) was used for the fabrication of stretchable armor by  
31 pouring it on a PMMA-coated silicon wafer after mixing with the curing agent. Then,  
32 spin-casting at 200 rpm generated a temporary substrate as a support for a sheet of  
33 fiberglass epoxy placed on top. Finally, the cleaning was done with laser cutting and  
34 isopropyl alcohol, and the scales and substrate were connected together [88].  
3536  
37 **5. Advances in analytical and computational modeling**  
3839 Fish scale inspired systems have diverse and often unique material design challenges.  
40 First, the combination of materials and geometry pose a combinatoric design space  
41 of vast parameters. In addition, the contact mechanics of scales make the problem  
42 highly nonlinear even for small strains. These periodic nonlinearities can result in  
43 unprecedented emergent behavior in dynamic loads, presence of friction, or cross  
44 curvature coupling. Therefore, simple hand calculations or strength of material type  
45 approach is insufficient to understand, design or optimize these systems. At the  
46 same time, high contrast of material behavior between the substrate and scales, large  
47 number of contacts and geometric nonlinearity of the slender substrate pose substantial  
48 challenges to traditional FE. Thus, modeling and simulation form an equally significant  
49

1  
2 *Biomimetic and Bioinspiration* 21  
34  
5 part of fish scale research. One of the earliest simulation studies related to fish scales  
6 has been done by Bruet et al. (2008) using finite element analysis (FEA) to develop  
7 a computational model for comparing the indentation modulus and yield stress of  
8 individual ganoid scales with experimental results and found it almost similar between  
9 the simulation and experimental data [24]. The authors described the mechanistic  
10 origins of penetration resistance as the juxtaposition of multiple distinct reinforcing  
11 composite layers in a ganoid scale. Therefore, each of these layers undergo their own  
12 unique deformation mechanisms under the penetrative load, and functionally gradation  
13 in mechanical properties of different regions of the scale [24].  
1415  
16 In another early research, Zhu et al. [65, 66] studied the puncture resistance  
17 of scaled skin from striped bass as an inspiration for flexible wearable armor under  
18 experimental efforts. They also developed an axisymmetric finite element model with  
19 a bilayer scale to model the outer bony layer and the softer collagen layer of the scales  
20 and studied the effect of scales pattern and friction between the scales under a local  
21 indentation load. It observed that the surrounding scales contribute to redistribute the  
22 puncture force over a larger area to limit local penetrative deflections in the soft tissues  
23 [66]. Also, the analytical “Four Flaps” model has been developed to describe crack  
24 failure in the bony layer of the scales [65]. By developing the bioinspired analogues of fish  
25 scales, this field of interest has been extended from studying natural scales to fabricated  
26 bioinspired composites and metamaterials [4, 20, 22, 25, 94]. In the earlier prototypes,  
27 the scales were considered fully embedded [20–22]. Through experimental analysis and  
28 numerical simulations for these kinds of prototypes, some protective mechanisms have  
29 been observed in the biomimetic scales composite, including the scale bending, scale  
30 rotation, and shear and constraint in the substrate [20]. Also, this protective response  
31 can be tailored by geometrical parameters including scale’s angle, scale’s overlap ratio,  
32 scale’s volume fraction, aspect ratio of the scales, and material properties of scales and  
33 substrate [20]. Also for fully embedded scale composites, exact analytical solutions were  
34 developed under compressive and bending loads with finite deformation assumption [21],  
35 which leads to rigorous response tailorability with respect to geometrical parameters  
36 similar to earlier study on fully embedded scale composites [21].  
3738  
39 In addition to the fully embedded scales composites, the exposed biomimetic scales  
40 metamaterials have been studied as well [4, 6, 12, 25, 94, 129, 130]. Exposed scales  
41 can be plate like, placed horizontally on a substrate [17, 25, 67, 94, 95, 99, 129], or  
42 partially embedded protruding scales [4–7, 12–14, 16]. In the exposed scales system, at  
43 a certain deformation of the substrate, the exposed parts of the scales start to contact  
44 or engage with each other. This engagement will add geometrical nonlinearity to the  
45 system leading to additional stiffening of the system. These large number of contact pairs  
46 through the whole biomimetic scale system and significant contact nonlinearity cause  
47 limitation in the commercial FE software for the convergence of numerical solution and  
48 critically reduce the speed of simulation. Therefore, in addition to the need for major  
49 advances in numerical modeling, analytical modeling is of importance, which can acquit  
50 the need for numerical simulations.  
51  
52  
53  
54  
55  
56  
57  
58  
59  
60

1  
2 *Biomimetic and Bioinspiration* 22  
34  
5 A basic micromechanical model, which correlate the flexural response, material  
6 properties of the substrates and the geometrical parameters of the scaled skin was  
7 introduced assuming periodic engagement[129]. This study revealed that scaled  
8 structures present inherent strain-stiffening response, which can be tailored by the scales  
9 design, scales spatial density, scale-dermis attachment stiffness, scales arrangement or  
10 pattern, and their material properties. They also find that in the absence of rigidity  
11 assumption for the scales, the scale's shear deformation makes reduction in the average  
12 stiffness and strain-stiffening characteristics of the scaled structure [129]. In another  
13 later study [17], they improved the introduced micromechanical model by establishing  
14 a more rigorous geometrical model between scales rotation and skin curvature. They  
15 also investigated the stiffening response of a scaled structure under buckling analysis  
16 in addition to the pure bending deformation. This investigation was resulted in the  
17 enhancing role of rigid scales to postpone the critical buckling load of the structure due  
18 to the resistance of the scales against out-of-plane rotation [17].  
19  
2021  
22 In other research works [4, 5, 16] a biomimetic scales metamaterial was considered  
23 with equally spaced rigid scales, which partially embedded on a deformable substrate,  
24 as shown in Figure 9 (a) that also developed specific rotational stiffness relationships.  
25 By assuming periodicity in scale engagement after bending deformation, the authors  
26 established a kinematic micro-model for the representative volume element (RVE) level,  
27 between the scale's inclination angle  $\theta$  and the substrate's local bending angle  $\psi$ , as  
28 follows:  
29  
30

31  
32 
$$\eta\psi \cos \psi/2 - \sin(\theta + \psi/2) = 0 \quad (1)$$
  
33  
34

35  
36 Here,  $d$ ,  $l$ ,  $\eta = l/d$ , and  $\kappa = \psi/d$  are the scales spacing, scales exposed length,  
37 scales overlap ratio, and beam curvature, respectively [4, 5]. This nonlinear relationship  
38 leads to a kinematic performance map as shown in Figure 9 (b), with three regimes of  
39 operations: (1) Linear performance before the scale engagement (horizontal section of  
40 each  $\eta$ 's curve). (2) Nonlinear stiffening after the scale engagement (ascending curved  
41 section of each  $\eta$ 's curve). (3) Kinematic locking, which is the singular point of equation  
42 (1) for each  $\eta$ 's curve and connecting these points for all curves leads to the kinematic  
43 locking border (black line in Figure 9 (b)).  
44  
4546 Then, by developing a micro-macro energy balance (Hill-Mandel Condition)  
47 [15, 131], the coupling between the kinematic and mechanic model has been established,  
48 which leads to the moment-curvature response of the system as shown in Figure 9 (c).  
49 These studies revealed that the frictionless scales engagement will add highly nonlinear  
50 stiffening to the system, which at a certain curvature will leads to the kinematic locking  
51 of system. Kinematic locking is because that further deformation in the system needs  
52 excessive deformation in the scales, which is against the rigidity of scales. They also  
53 showed that the friction force between the scales has a dual contribution including  
54 advancing the locking mechanism by changing the mechanism depending on purely  
55 kinematic configuration to the interfacial behavior, and stiffening the bending moment  
56 response due to the increase in the engagement forces [5].  
57  
58  
59  
60

## Biomimetic and Bioinspiration

23

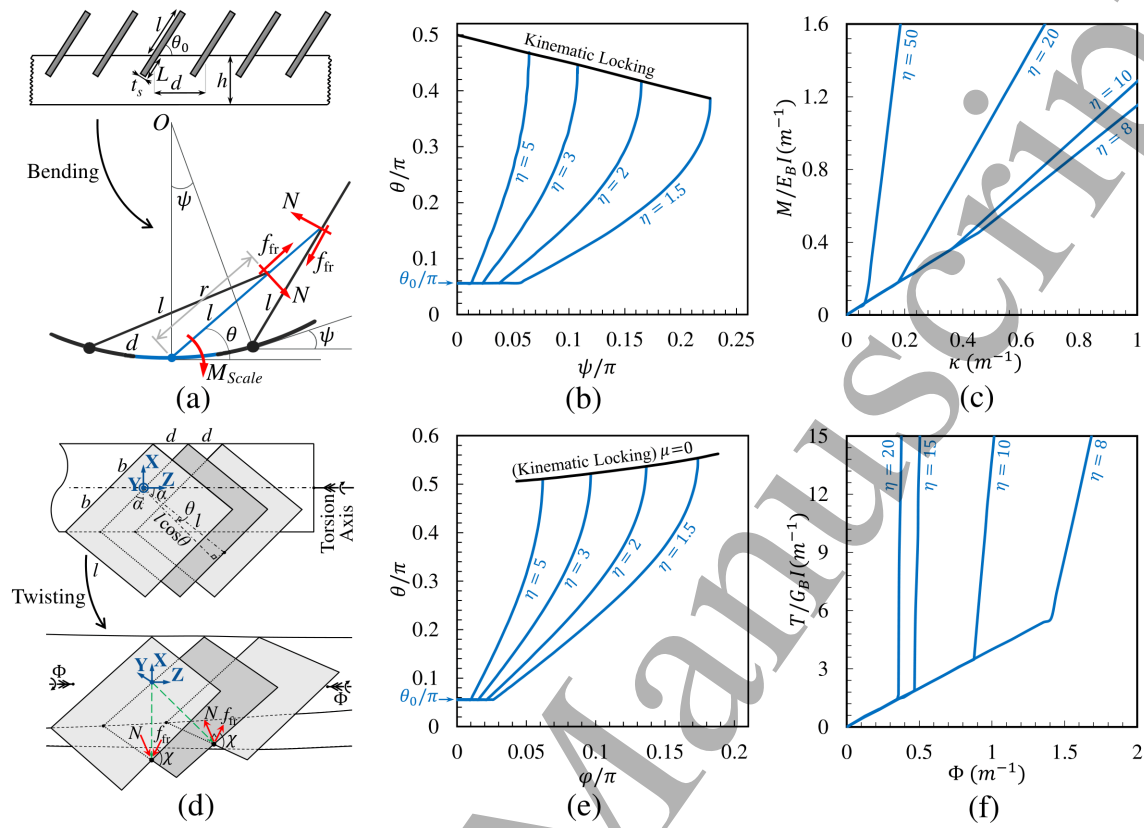


**Figure 9.** (a) Isolated RVE and free body diagram for bending case. (b) Kinematic performance map for bending case. (c) Moment–curvature response for bending case. (d) Isolated RVE and free body diagram for twisting case. (e) Kinematic performance map for twisting case. (f) Torque–twist rate response for twisting case.

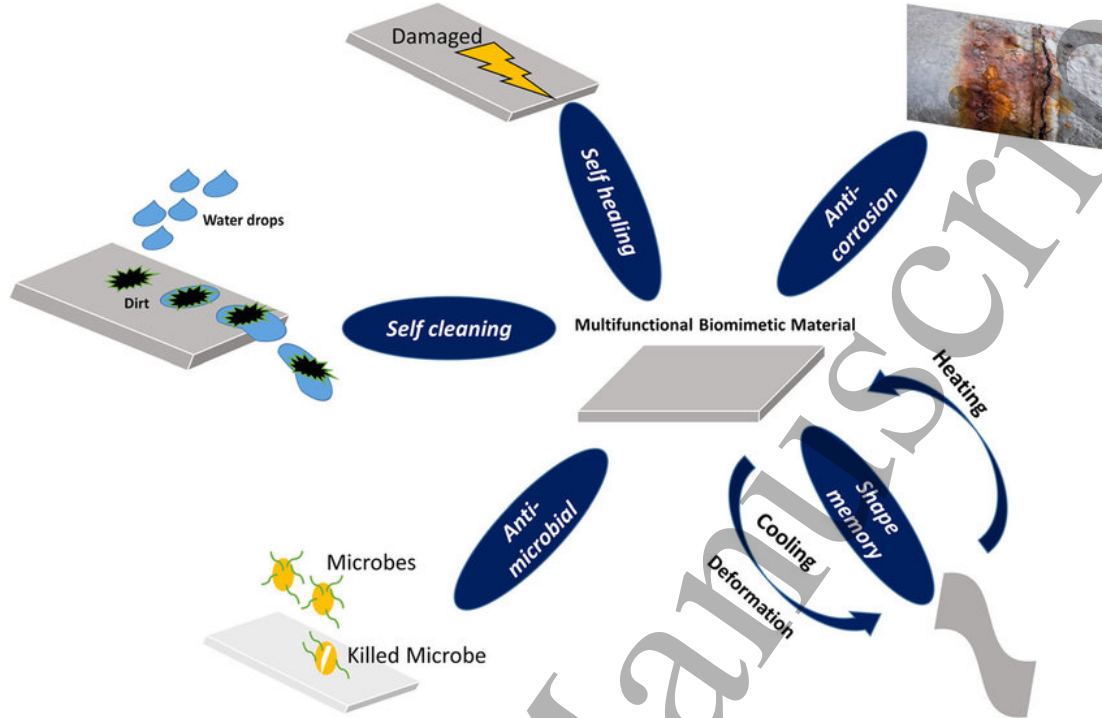
Later researches [12, 14, 16] revealed that the essential characteristics of a scaled structure under bending deformation including strain stiffening, and the locked condition are universally valid even when the scales are not rigid [16, 129], or when periodicity is not valid as scales are not uniformly distributed (e.g. functionally graded [14]) or loading is not uniform bending [12]. For when the periodicity is not satisfied, a discrete non-periodic model have been developed instead of equation (1) [12, 14]. Recent studies in twisting of biomimetic scales have also indicated the universality of locking and strain stiffening under pure torsion [6, 7]. For the twisting case, scales are considered with oblique angle  $\alpha$  with respect to the torsion axis (in addition to the inclination angle  $\theta$  with respect to the substrate surface) [6], as shown in the RVE in Figure 9 (d). This is because that in early studies on the scaled system under twisting, no significant stiffening was indicated despite the bending case for the scales arrangement as parallel to the torsion axis [67]. However, there are striking differences between bending and twisting. For instance, the kinematic locking border is nonlinear functions of geometry as shown in Figure 9 (e), unlike the bending case which is linear as shown in Figure 9 (b). Moreover, the torque–twist response of the system has been shown in Figure 9 (f). By including the friction for twisting case [7], frictional locking is found universal as well,

1  
2 *Biomimetic and Bioinspiration*  
3  
4

24

5 but as a highly nonlinear curve, without any closed form solution, unlike the bending  
6 case. Also, in the twisting, the relative energy dissipation is increasing monotonically  
7 with  $\mu$ , which in the bending case increasing in the  $\mu$  may not necessarily increase the  
8 relative energy dissipation of the system [5, 7].  
910 Most of these studies for modeling or simulation of biomimetic scaled systems are  
11 under static loads including indentation, bending, and twisting. There are limited  
12 studies on the modeling or simulation of dynamic loading on biomimetic scales systems  
13 [13, 130, 132]. Liu et al. [130] developed biomimetic composite scale to investigate under  
14 ballistic impact, by inspiration from the two-layer structure and overlapping pattern of  
15 fish scales using silicon carbide (SiC) ceramic as the outer layer, and aluminum as the  
16 inner layer of the scales, respectively. Through the numerical simulation, they found the  
17 optimal thickness ratio of SiC/Al to reduce the area density of bio-inspired composite  
18 scale with the same ballistic performance at a certain impact velocity. Additionally, with  
19 a comparative simulation analysis with of overlapped bioinspired composite scales, an  
20 optimal overlapping ratio has been discovered [130]. Recently, the emergent dynamical  
21 behavior in a biomimetic scaled system has been studied using the variational energy  
22 equation, delivered from Hamilton principle for a simply supported scaled beam with  
23 initial velocity condition [13]. The equation of motion has been solved numerically using  
24 the direct numerical integration method. The free oscillation response shows that the  
25 system oscillates with exponential decay due to the interfacial friction between scales,  
26 unlike the spring-mass system with dry friction, which indicates a linear decay. In  
27 scaled biomimetic system, the decay will not lead to a totally damping mode unlike  
28 the conventional damped oscillation, but it continues rather until the deflection is  
29 small enough when the scales don't engage anymore [13]. Also, few recent studies  
30 [132, 133] have been studied numerically the ballistic behavior of bioinspired ceramic  
31 armors based on ganoid and placoid fish scales. The main conclusion is related to  
32 the improved efficiency of a modular armor against multiple shots exhibiting more  
33 localized damage and crack arrest properties. Moreover, its potential ergonomic is  
34 a promising characteristic justifying a deeper study. These modular armors showed  
35 improved efficiency against multiple ballistic shots by providing more localized damage  
36 and crack arrest behavior [132].  
37  
38  
39  
40  
41  
42  
43  
44  
4546  
47 **6. Conclusions, challenges, and future outlook**  
48  
4950 In spite of impressive advances covering design, fabrication and simulations, several  
51 gaps and scope for new scientific discoveries remain. For example, still relatively little  
52 is known about the behavior of scale-covered 2D systems like a scale-covered plate and  
53 shell systems with more general variations scale geometry, distribution, scale surface  
54 morphology and material properties. Also in spite of early advances in using shark  
55 skin concept for drag reduction [101, 128], the fluid structure interaction of flow with  
56 property programmable scales are relatively unexplored. One of the major challenges  
57 remain understanding the multiple-scale fluid-structure interaction problem specific to  
58  
59  
60

1  
2 *Biomimetic and Bioinspiration* 25  
34  
5 these problems. The recent work on buckling behavior [94, 134], also points to potential  
6 future research on the enriching effects of the scales geometry and nonuniform scales  
7 distribution to reach to additional buckling modes and generating localized deformation  
8 as combinations of deformation and constraints [94, 126].  
910 Furthermore, nearly all discussed works on the biomimetic scales systems, consider  
11 perfectly bonded scales on the substrate, and the substrate without any imperfections.  
12 Other than some previous work exploring this topic [16], much more is needed to quantify  
13 the effects of imperfections of the substrate or bonding of the scales with the substrate.  
14 Such knowledge could be effective for the additional tailorability of material response  
15 [94, 134]. The bonding of the scales with substrates is often done using powerful glues.  
16 The strength of this bond is critical towards enhancing the overall performance of this  
17 system. Such bonding can also be improved using mechanical joints or hierarchical  
18 root-like topology. Such joints engineering is an important area of further development.  
1920 Mechanics and dynamics behavior of 2D scales such as scales distribution,  
21 synergistic behavior, and metamaterials behavior under different load conditions is one  
22 of the major field for future scope. Time dependent behavior of biomimetic scales  
23 is also one of the promising filed that need to be investigated to understand the  
24 time dependent properties of dynamically changing scales structure [15]. Also, less  
25 explored is development of multi-functional biomimetic surface, which can include self-  
26 repairing and self-cleaning behavior, mechanically and chemically protective coatings,  
27 and advanced optical properties. For example, shark skin, which has some topological  
28 surface features like scales, has self-cleaning properties and low fluid drag behavior, and  
29 these novel properties could be applicable to coating of the aircraft fuselage and the hull  
30 of ship. Very few studies have been conducted in the past focusing on this aspect, even  
31 though this can increase the usage of biomimetic fish scales in various emerging sectors  
32 [135–138]. Among various advantages of teleost fish scales, they have such mechanical  
33 properties that prevent from penetration. Even, the scales of *Archispirostreptus gigas*  
34 provide protection against counter ballistic projectile from smaller bullets [1, 139, 140].  
35 In future the development of rapid prototyping technology may allow the 3D printing of  
36 microstructure of scales with desired mechanical properties that can widen the use and  
37 performance of biomimetic fish scales [1]. The schematic diagram summarizing such  
38 possibilities is shown in figure 10 [137].  
3940 Numerical simulations of these metmaterials have encountered some limitations of  
41 the commercial FE software because of to the large number of contact pairs between  
42 the scales and the significant contact nonlinearity brought to the FE models. Therefore,  
43 major advance in numerical simulations and multiscale modeling is needed [15]. Also,  
44 other novel behaviors can be obtained by using the phase change materials as tailorabile  
45 stiffening scales, and color changing materials to provide unprecedented on-demand  
46 change of stiffness and optical response as a functional programmability properties  
47 [96, 141]. It seems that there are no significant number of research on this type of time  
48 dependent behavior and dynamically changing scales systems, because of the necessary  
49 needs of advancement in the fabrication techniques and multiphysics modeling. Also,  
50

1  
2 *REFERENCES*  
3  
4  
5  
6  
7  
8  
9  
10  
11  
12  
13  
14  
15  
16  
17  
18  
19  
20  
21  
22  
23  
24  
25  
26  
27  
28  
29  
30  
31  
32  
33  
34  
35  
36  
37  
38  
39  
40  
41  
42  
43  
44  
45  
46  
47  
48  
49  
50  
51  
52  
53  
54  
55  
56  
57  
58  
59  
60

**Figure 10.** Schematic diagram showing the possible integration of multiple biomimetic functionality [137]. (Copyright permission has been adopted.)

studies on the thermal or electromagnetic behavior of these metamaterials have not been considered yet, which could be a key future frontier in this field. Such complexities in the material, fabrication, and modeling of these system can give rise to new and potentially unanticipated challenges, which is needed to be addressed in future efforts.

### Acknowledgements

This work was supported by the United States National Science Foundation's Civil, Mechanical, and Manufacturing Innovation, CAREER Award #1943886, and #2028338.

### References

- [1] Yaseen A A, Waqar T, Khan M A A, Asad M and Djavanroodi F 2021 *Frontiers in Materials* **8** 114
- [2] Wang B, Yang W, Sherman V R and Meyers M A 2016 *Acta biomaterialia* **41** 60–74
- [3] Mirkhalaf M, Tanguay J and Barthelat F 2016 *Extreme Mechanics Letters* **7** 104–113
- [4] Ghosh R, Ebrahimi H and Vaziri A 2014 *Applied Physics Letters* **105** 233701
- [5] Ghosh R, Ebrahimi H and Vaziri A 2016 *EPL (Europhysics Letters)* **113** 34003

1  
2 *REFERENCES*  
3  
4

27

5 [6] Ebrahimi H, Ali H, Horton R A, Galvez J, Gordon A P and Ghosh R 2019 *EPL (Europhysics Letters)* **127** 24002

6 [7] Ebrahimi H, Ali H and Ghosh R 2020 *Bioinspiration & Biomimetics* **15** 056013

7 [8] Fish U and Region W S S 2010 (accessed May 19, 2022) Albino alligator gars,  
8 online Image, Flickr, <https://flic.kr/p/9rUgZ>

9 [9] Krejci K 2009 (accessed May 19, 2022) Alligator gar, online Image, Flickr,  
10 <https://flic.kr/p/6sMek1>

11 [10] Lian Z, Xu J, Wan Y, Li Y, Yu Z, Liu Q and Yu H 2017 *Materials Research Express* **4** 106504

12 [11] Ebrahimi H, Ali H, Stephen J, Dharmavaram S and Ghosh R 2021 Emergent  
13 mechanical properties of biomimetic exoskeletal metamaterials *Bioinspiration,  
14 Biomimetics, and Bioreplication XI* vol 11586 (International Society for Optics  
15 and Photonics) p 115860N

16 [12] Ali H, Ebrahimi H and Ghosh R 2019 *International Journal of Solids and  
17 Structures* **166** 22–31

18 [13] Ali H, Ebrahimi H and Ghosh R 2019 *Scientific reports* **9** 1–7

19 [14] Ali H, Ebrahimi H and Ghosh R 2019 *Mechanics of Soft Materials* **1** 1–12

20 [15] Ebrahimi H, Ali H, Stephen J and Ghosh R 2021 *EPL (Europhysics Letters)* **133**  
21 68001

22 [16] Ghosh R, Ebrahimi H and Vaziri A 2017 *Journal of the mechanical behavior of  
23 biomedical materials* **72** 1–5

24 [17] Vernerey F J and Barthelat F 2014 *Journal of the Mechanics and Physics of Solids*  
25 **68** 66–76

26 [18] White Z W 2018 *Fish-Scales: The Next Step in Soft Body Protection?* Ph.D.  
27 thesis University of Colorado at Boulder

28 [19] du Plessis A and Broeckhoven C 2019 *Acta biomaterialia* **85** 27–40

29 [20] Browning A, Ortiz C and Boyce M C 2013 *Journal of the mechanical behavior of  
30 biomedical materials* **19** 75–86

31 [21] Rudykh S and Boyce M C 2014 *IMA Journal of Applied Mathematics* **79** 830–847

32 [22] Rudykh S, Ortiz C and Boyce M C 2015 *Soft Matter* **11** 2547–2554

33 [23] Dien A E 2000 *Journal of East Asian Archeaology* 2–3

34 [24] Bruet B J, Song J, Boyce M C and Ortiz C 2008 *Nature materials* **7** 748–756

35 [25] Martini R, Balit Y and Barthelat F 2017 *Acta biomaterialia* **55** 360–372

36 [26] Ehrlich H 2015 Materials design principles of fish scales and armor *Biological  
37 Materials of Marine Origin* (Springer) pp 237–262

38 [27] White Z W and Vernerey F J 2018 *Bioinspiration & biomimetics* **13** 041004

39 [28] Kumari S and Rath P K 2014 *Procedia Materials Science* **6** 482–489

40

41

42

43

44

45

46

47

48

49

50

51

52

53

54

55

56

57

58

59

60

1  
2 *REFERENCES*  
3  
4

28

[29] Allison P G, Chandler M, Rodriguez R, Williams B, Moser R, Weiss Jr C, Poda A, Lafferty B, Kennedy A, Seiter J *et al.* 2013 *Acta biomaterialia* **9** 5289–5296

[30] Ikoma T, Kobayashi H, Tanaka J, Walsh D and Mann S 2003 *Journal of structural biology* **142** 327–333

[31] Nagai T, Izumi M and Ishii M 2004 *International journal of food science & technology* **39** 239–244

[32] Ryou H, Pashley D H, Tay F R and Arola D 2013 *Dental Materials* **29** 719–728

[33] Dharmavaram S, Ebrahimi H and Ghosh R 2022 *Journal of the Mechanics and Physics of Solids* **159** 104711

[34] Quan H, Yang W, Lapeyriere M, Schaible E, Ritchie R O and Meyers M A 2020 *Matter* **3** 842–863

[35] Quan H, Yang W, Tang Z, Ritchie R O and Meyers M A 2020 *Materials Today* **38** 35–48

[36] Naleway S E, Porter M M, McKittrick J and Meyers M A 2015 *Advanced materials* **27** 5455–5476

[37] Yang W, Naleway S E, Porter M M, Meyers M A and McKittrick J 2015 *Acta biomaterialia* **23** 1–10

[38] Wainwright D K 2019 *Fish scales: Morphology, evolution, and function* Ph.D. thesis Harvard University

[39] Zhu D, Zhang C, Liu P and Jawad L A 2019 *Journal of Bionic Engineering* **16** 328–336

[40] Jawad L A 2005 *Journal of Natural History* **39** 2643–2660

[41] Onozato H and Watabe N 1979 *Cell and tissue research* **201** 409–422

[42] Zylberberg L and Nicolas G 1982 *Cell and tissue research* **223** 349–367

[43] Zylberberg L, Bonaventure J, Cohen-Solal L, Hartmann D and Bereiterhahn J 1992 *Journal of Cell Science* **103** 273–285

[44] Giraud-Guille M M, Besseau L, Chopin C, Durand P and Herbage D 2000 *Biomaterials* **21** 899–906

[45] Mathews M B 1975 Polyanionic proteoglycans *Connective Tissue* (Springer) pp 93–125

[46] Ashwitha A, Thamizharasan K and Bhatt P 2020 *SN Applied Sciences* **2** 1–8

[47] Kara A, Gunes O C, Albayrak A Z, Bilici G, Erbil G and Havitcioglu H 2020 *Journal of biomaterials applications* **34** 1201–1215

[48] Nagai T, Suzuki N and Nagashima T 2008 *Food chemistry* **111** 296–301

[49] Wu W, Zhou Z, Sun G, Liu Y, Zhang A and Chen X 2021 *Materials Science and Engineering: C* **122** 111919

[50] Ikoma T, Kobayashi H, Tanaka J, Walsh D and Mann S 2003 *International journal of biological macromolecules* **32** 199–204

1  
2 *REFERENCES*  
3  
4

29

5 [51] Long J, Hale M, McHenry M and Westneat M 1996 *The Journal of experimental*  
6 *biology* **199** 2139–2151

7 [52] Chen W, Zhang H, Huang Y and Wang W 2010 *Journal of Materials Chemistry*  
8 **20** 4773–4775

9 [53] Feng H, Li X, Deng X, Li X, Guo J, Ma K and Jiang B 2020 *Rsc Advances* **10**  
10 875–885

11 [54] Song J, Reichert S, Kallai I, Gazit D, Wund M, Boyce M C and Ortiz C 2010  
12 *Journal of structural biology* **171** 318–331

13 [55] Zimmermann E A, Gludovatz B, Schaible E, Dave N K, Yang W, Meyers M A  
14 and Ritchie R O 2013 *Nature communications* **4** 1–7

15 [56] Varshney S, Song J, Li Y, Boyce M C and Ortiz C 2015 *Journal of structural*  
16 *biology* **192** 487–499

17 [57] Garrano A M C, La Rosa G, Zhang D, Niu L N, Tay F, Majd H and Arola D 2012  
18 *Journal of the mechanical behavior of biomedical materials* **7** 17–29

19 [58] Fu Z, Ma W, Zhu T, Ye P and Li G 2020 Measurement of mechanical properties  
20 of carp scales based on digital image correlation method *Journal of Physics: Conference Series* vol 1605 (IOP Publishing) p 012107

21 [59] Jiang H, Ghods S, Weller E, Waddell S, Ossa E, Yang F and Arola D 2020 *Acta*  
22 *biomaterialia* **106** 242–255

23 [60] Ghods S, Murcia S, Ossa E and Arola D 2019 *Journal of the mechanical behavior*  
24 *of biomedical materials* **90** 451–459

25 [61] Arola D, Ghods S, Son C, Murcia S and Ossa E 2019 *Journal of the Royal Society*  
26 *Interface* **16** 20180775

27 [62] Lin Y, Wei C, Olevsky E and Meyers M A 2011 *Journal of the mechanical behavior*  
28 *of biomedical materials* **4** 1145–1156

29 [63] Nelms M, Hodo W and Rajendran A 2017 *Journal of the mechanical behavior of*  
30 *biomedical materials* **69** 395–403

31 [64] Lin A 2017 *Design of flexible puncture resistant gloves inspired by natural dermal*  
32 *armors* Ph.D. thesis University of Washington

33 [65] Zhu D, Ortega C F, Motamedi R, Szewciw L, Vernerey F and Barthelat F 2012  
34 *Advanced Engineering Materials* **14** B185–B194

35 [66] Zhu D, Szewciw L, Vernerey F and Barthelat F 2013 *Journal of the mechanical*  
36 *behavior of biomedical materials* **24** 30–40

37 [67] Vernerey F J, Musiket K and Barthelat F 2014 *International Journal of Solids*  
38 *and Structures* **51** 274–283

39 [68] Ghods S, Waddell S, Weller E, Renteria C, Jiang H Y, Janak J, Mao S, Linley T  
40 and Arola D 2020 *Journal of Experimental Biology* **223** jeb211144

1  
2 *REFERENCES*  
3  
4

30

[69] Yang W, Sherman V R, Gludovatz B, Mackey M, Zimmermann E A, Chang E H, Schaible E, Qin Z, Buehler M J, Ritchie R O *et al.* 2014 *Acta biomaterialia* **10** 3599–3614

[70] Rawat P, Liu P, Zhang C, Guo S, Jawad L A, Sadighzadeh Z and Zhu D 2021 *Journal of fish biology*

[71] Nadeem R, Ansari T M and Khalid A M 2008 *Journal of Hazardous Materials* **156** 64–73

[72] Liu Z, Zhang Z and Ritchie R O 2020 *Acta Biomaterialia* **102** 75–82

[73] Chen I H, Kiang J H, Correa V, Lopez M I, Chen P Y, McKittrick J and Meyers M A 2011 *Journal of the mechanical behavior of biomedical materials* **4** 713–722

[74] Hubbard R P, Melvin J W and Barodawala I T 1971 *Journal of biomechanics* **4** 491–496

[75] Fratzl P, Kolednik O, Fischer F D and Dean M N 2016 *Chemical Society Reviews* **45** 252–267

[76] Herring S W 2008 *Craniofacial sutures* **12** 41–56

[77] Chon M J, Daly M, Wang B, Xiao X, Zaheri A, Meyers M A and Espinosa H D 2017 *Journal of the mechanical behavior of biomedical materials* **76** 30–37

[78] Liu Z, Jiao D, Weng Z and Zhang Z 2016 *Journal of the mechanical behavior of biomedical materials* **56** 165–174

[79] Häsä R and Pinho S 2020 *Materials Letters* **273** 127966

[80] White Z, Shen T, Volk E M and Vernerey F J 2019 *Mechanics Research Communications* **98** 1–8

[81] Ehrlich H 2010 *Biological materials of marine origin* (Springer)

[82] Stephen J 2020 *Contact mechanics of fish scale inspired exoskeletal components on a nonlinear elastic substrate* Master's thesis University of Central Florida

[83] Johnson A, Bingham G A and Wimpenny D I 2013 *Rapid Prototyping Journal*

[84] Johnson A, Bingham G and Majewski C E 2018 *Virtual and Physical Prototyping* **13** 49–57

[85] Johnson A 2014 *Establishing design characteristics for the development of stab resistant Laser Sintered body armour* Ph.D. thesis Loughborough University

[86] Martini R and Barthelat F 2016 *Journal of the Mechanics and Physics of Solids* **92** 195–209

[87] Funk N, Vera M, Szewciw L J, Barthelat F, Stoykovich M P and Vernerey F J 2015 *ACS applied materials & interfaces* **7** 5972–5983

[88] Choi J, Han S, Baliwag M, Kim B H, Jang H, Kim J T, Hong I, Kim T, Kang S M, Lee K T *et al.* 2021 *Extreme Mechanics Letters* 101537

[89] Zheng Y, Guo C and Li X 2021 *Materials Research Express* **8** 035014

[90] Estrada S and Ossa A 2020 *Advanced Engineering Materials* **22** 2000006

1  
2 *REFERENCES*  
3  
4

31

5 [91] Mirkhalaf M, Zhou T and Barthelat F 2018 *Proceedings of the National Academy of Sciences* **115** 9128–9133

6 [92] Chintapalli R K, Mirkhalaf M, Dastjerdi A K and Barthelat F 2014 *Bioinspiration & biomimetics* **9** 036005

7 [93] Martini R and Barthelat F 2016 *Bioinspiration & biomimetics* **11** 066001

8 [94] Shafiei A, Pro J W and Barthelat F 2021 *Bioinspiration & Biomimetics*

9 [95] Shafiei A, Pro J W, Martini R and Barthelat F 2021 *Journal of the Mechanics and Physics of Solids* **146** 104176

10 [96] Tatari M, Kamrava S, Ghosh R, Nayeb-Hashemi H and Vaziri A 2020 *Scientific reports* **10** 1–8

11 [97] Ali H, Ebrahimi H, Stephen J, Warren P and Ghosh R 2020 Tailorable stiffness  
12 lightweight soft robotic materials with architectured exoskeleton *AIAA Scitech  
2020 Forum* p 1551

13 [98] Han X, Zhang D, Li X and Li Y 2008 *Chinese Science Bulletin* **53** 1587–1592

14 [99] Liu M, Wang S, Wei Z, Song Y and Jiang L 2009 *Advanced Materials* **21** 665–669

15 [100] Muthuramalingam M, Puckert D K, Rist U and Bruecker C 2020 *Scientific Reports*  
16 **10** 1–13

17 [101] Wang Y, Zhang Z, Xu J and Yu H 2021 *Surface and Coatings Technology* **409**  
18 126801

19 [102] Wen L, Weaver J C and Lauder G V 2014 *Journal of Experimental Biology* **217**  
20 1656–1666

21 [103] Oeffner J and Lauder G V 2012 *Journal of Experimental Biology* **215** 785–795

22 [104] Nishimoto S and Bhushan B 2013 *Rsc Advances* **3** 671–690

23 [105] Liu K, Yao X and Jiang L 2010 *Chemical Society Reviews* **39** 3240–3255

24 [106] Bixler G D and Bhushan B 2012 *Soft matter* **8** 11271–11284

25 [107] Sun Y and Guo Z 2019 *Nanoscale Horizons* **4** 52–76

26 [108] Bixler G D and Bhushan B 2013 *Soft Matter* **9** 1620–1635

27 [109] Islam M K, Hazell P J, Escobedo J P and Wang H 2021 *Materials & Design*  
28 109730

29 [110] Mirkhalaf M, Sunesara A, Ashrafi B and Barthelat F 2019 *International Journal  
30 of Solids and Structures* **158** 52–65

31 [111] Duro-Royo J, Zolotovsky K, Mogas-Soldevila L, Varshney S, Oxman N, Boyce  
32 M C and Ortiz C 2015 *Computer-Aided Design* **60** 14–27

33 [112] Landreneau E B 2011 *Scales and scale-like structures* (Texas A & M University)

34 [113] Robinson H R 1975 *The armour of imperial Rome* (Scribner)

35 [114] She W, Wang X, Miao C, Zhang Q, Zhang Y, Yang J and Hong J 2018  
36 *Construction and Building Materials* **181** 347–357

37  
38  
39  
40  
41  
42  
43  
44  
45  
46  
47  
48  
49  
50  
51  
52  
53  
54  
55  
56  
57  
58  
59  
60

1  
2 *REFERENCES*  
3  
4

32

[115] Krogman K, Cohen R, Hammond P, Rubner M and Wang B 2013 *Bioinspiration & biomimetics* **8** 045005

[116] Yang Y, Song X, Li X, Chen Z, Zhou C, Zhou Q and Chen Y 2018 *Advanced Materials* **30** 1706539

[117] Du Plessis A, Broeckhoven C, Yadroitsava I, Yadroitsev I, Hands C H, Kunju R and Bhate D 2019 *Additive Manufacturing* **27** 408–427

[118] Snell-Rood E 2016 *Nature News* **529** 277

[119] Porter M M, Ravikumar N, Barthelat F and Martini R 2017 *Journal of the mechanical behavior of biomedical materials* **73** 114–126

[120] Yan X, Chen H, Lin S, Xiao S and Yang Y 2021 *Frontiers in Materials* **8** 139

[121] Ebrahimi H 2021 *Mechanics of Low Dimensional Biomimetic Scale Metamaterials* Ph.D. thesis University of Central Florida

[122] Reichert S H 2010 *Reverse engineering nature: design principles for flexible protection inspired by ancient fish armor of Polypteridae* Ph.D. thesis Massachusetts Institute of Technology

[123] Yasuda Y, Zhang K, Sasaki O, Tomita M, Rival D and Galipon J 2019 *Journal of The Electrochemical Society* **166** B3302

[124] Chen A, Thind K, Demir K G and Gu G X 2021 *Materials* **14** 5378

[125] Johnson A, Bingham G A and Majewski C E 2015 *International Journal of Rapid Manufacturing* **5** 3–19

[126] Connors M, Yang T, Hosny A, Deng Z, Yazdandoost F, Massaadi H, Eernisse D, Mirzaeifar R, Dean M N, Weaver J C et al. 2019 *Nature communications* **10** 1–13

[127] Ali H 2021 *The Mechanics and Multiphysics of Biomimetic Discrete Exoskeleton Substrates* Ph.D. thesis University of Central Florida

[128] Dean B and Bhushan B 2010 *Philosophical Transactions of the Royal Society A: Mathematical, Physical and Engineering Sciences* **368** 4775–4806

[129] Vernerey F J and Barthelat F 2010 *International Journal of Solids and Structures* **47** 2268–2275

[130] Liu P, Zhu D, Yao Y, Wang J and Bui T Q 2016 *Materials & Design* **99** 201–210

[131] Nemat-Nasser S and Hori M 2013 *Micromechanics: overall properties of heterogeneous materials* (Elsevier)

[132] González-Albuixech V F, Rodríguez-Millán M, Ito T, Loya J and Miguélez M 2019 *International Journal of Damage Mechanics* **28** 815–837

[133] Zhang C, Rawat P, Liu P and Zhu D 2020 *Bioinspiration & Biomimetics* **15** 066003

[134] Budiansky B and Hutchinson J W 1966 Dynamic buckling of imperfection-sensitive structures *Applied mechanics* (Springer) pp 636–651

[135] Zhou T, Sui B, Mo X and Sun J 2017 *International journal of nanomedicine* **12** 3495

1  
2        *REFERENCES*  
3  
4  
5  
6  
7  
8  
9  
10  
11  
12  
13  
14  
15  
16  
17  
18  
19  
20  
21  
22  
23  
24  
25  
26  
27  
28  
29  
30  
31  
32  
33  
34  
35  
36  
37  
38  
39  
40  
41  
42  
43  
44  
45  
46  
47  
48  
49  
50  
51  
52  
53  
54  
55  
56  
57  
58  
59  
60

[136] Sun Z, Liao T, Li W, Dou Y, Liu K, Jiang L, Kim S W, Kim J H and Dou S X 2015 *NPG Asia Materials* **7** e232–e232

[137] Vijayan P P and Puglia D 2019 *Emergent Materials* **2** 391–415

[138] Fu Y, Yuan C and Bai X 2017 *Biosurface and Biotribology* **3** 11–24

[139] Rawat P, Zhu D, Rahman M Z and Barthelat F 2021 *Acta Biomaterialia* **121** 41–67

[140] Liu J, Singh A, Lee H, Tay T and Tan V 2020 *International Journal of Impact Engineering* **142** 103608

[141] Kamrava S, Tatari M, Feng X, Ghosh R and Vaziri A 2019 *Advanced Intelligent Systems* **1** 1900021